AFOSR FINAL SCIENTIFIC REPORT

AFOSR TR-77-0696

RESPONSE OF STRUCTURES TO RANDOM NOISE

William A. Nash

November, 1976

UNIVERSITY OF MASSACHUSETTS

AIR FORCE OFFICE OF SCIENTIFIC RESEARCH
UNITED STATES AIR FORCE
GRANT NO. AFOSR 72-2340

AFOSR FINAL REPORT
TR-77-0696

RESPONSE OF STRUCTURES TO RANDOM NOISE

William A. Nash

November, 1976

UNIVERSITY OF MASSACHUSETTS

Air Force Office of Scientific Research
United States Air Force
Grant No. AFOSR 72-2340

ABSTRACT

The work reported here has been directed along three main avenues. First, a new method has been developed for determination of natural frequencies and associated mode shapes of thin elastic plates and also shallow shells undergoing free, undamped vibration. This method permits consideration of arbitrary boundary conditions along each side of a polygonal plate or polygonal plan-form shell and further offers a comprehensive evaluation of how well the boundary conditions have been satisfied along each edge. Second, the structural reliability of geometrically nonlinear structures subject to stationary random excitation has been investigated by two approaches which have been found to yield satisfactory predictions of reliability. Third, a technique has been developed for prediction of the statistical characteristics of the response of a nonlinear system to nonstationary random excitation.

REPORT DOCUMENTATION PAGE

READ INSTRUCTIONS BEFORE COMPLETING FORM

1. REPORT NUMBER: AFOSR TR-77-0696	2. GOVT ACCESSION NO.: ADA 040513
3. RECIPIENT'S CATALOG NUMBER:	
4. TITLE (and Subtitle): RESPONSE OF STRUCTURES TO RANDOM NOISE	5. TYPE OF REPORT & PERIOD COVERED: FINAL 1 Aug 72-31 Oct 76
	6. PERFORMING ORG. REPORT NUMBER:
7. AUTHOR(s): WILLIAM A NASH	8. CONTRACT OR GRANT NUMBER(s): AFOSR 72-2340
9. PERFORMING ORGANIZATION NAME AND ADDRESS: UNIVERSITY OF MASSACHUSETTS DEPARTMENT OF CIVIL ENGINEERING AMHERST, MA 01002	10. PROGRAM ELEMENT, PROJECT, TASK AREA & WORK UNIT NUMBERS: 681307 9782-01 61102F
11. CONTROLLING OFFICE NAME AND ADDRESS: AIR FORCE OFFICE SCIENTIFIC RESEARCH/NA BIDG 410 BOLLING AIR FORCE BASE, D C 20332	12. REPORT DATE: Nov 76
	13. NUMBER OF PAGES: 79
14. MONITORING AGENCY NAME & ADDRESS (if different from Controlling Office):	15. SECURITY CLASS. (of this report): UNCLASSIFIED
	15a. DECLASSIFICATION/DOWNGRADING SCHEDULE:

16. DISTRIBUTION STATEMENT (of this Report)

Approved for public release; distribution is unlimi[illegible].

17. DISTRIBUTION STATEMENT (of the abstract entered in Block 20, if different from Report)

18. SUPPLEMENTARY NOTES

19. KEY WORDS (Continue on reverse side if necessary and identify by block number)

RANDOM VIBRATIONS
PLATES
SHELLS
VIBRATIONS
STRUCTURAL RELIABILITY

20. ABSTRACT (Continue on reverse side if necessary and identify by block number)

The work reported here has been directed along three main avenues. First, a new method has been developed for determination of natural frequencies and associated mode shapes of thin elastic plates and also shallow shells undergoing free, undamped vibration. The method permits consideration of arbitrary boundary conditions along each side of a polygonal plate or polygonal plan-form shell and further offers a comprehansive evaluation of how well the boundary conditions have been satisfied along each edge. Second, the structural reliability of geometrically nonlinear structures subject to stationary random excitation has

been investigated by two approaches which have been found to yield satisfactory predictions of reliability. Third, a technique has been developed for prediction of the statistical characteristics of the response of a nonlinear system to nonstationary random excitation.

CHAPTER I

VIBRATIONS OF THIN ELASTIC PLATES

Introduction

Problems involving vibrations of thin, elastic plates occur in a wide variety of applications in structural mechanics in all aspects of engineering. An excellent comprehensive summary of existing analytical and experimental information pertinent to this problem area has recently been presented by A. W. Leissa [1].*

The present investigation, concerned with free vibrations of thin elastic plates is based upon the assumptions that (a) the thickness of the plate is small compared to its other dimensions, (b) there is no middle surface extension or contraction, (c) points situated on a line normal to the undeformed middle surface remain on this same line as the plate deforms during vibration, (d) stresses normal to the middle surface of the plate are neglected, and (e) Hooke's law is valid.

Many problems involving free vibrations of plates have been solved by exact methods, energy techniques, and various numerical approaches, in particular finite elements. The objective of the present work is to present a more generalized approach that is applicable to arbitrary plate contours and arbitrary boundary conditions. Also, it is desirable to present a method that decreases the computer effort involved in other approaches. With this in mind, the present work develops a dynamic analog of the Edge-Function method originally due to P. M. Quinlan [2] and applied successfully by him to a variety of elastostatic problems [3],[4] including static deflections of thin elastic plates [5] and [6].

*Numbers in brackets refer to references at the end of the text.

Governing Relationships

The fundamental differential equation of motion for the transverse displacement w of a plate is:

$$D\left[\frac{\partial^4 w}{\partial x^4} + 2\frac{\partial^4 w}{\partial x^2 \partial y^2} + \frac{\partial^4 w}{\partial y^4}\right] + \rho\frac{\partial^2 w}{\partial t^2} = 0 \qquad (I\text{-}1)$$

where the deflection w (x,y,t) is a function of the rectangular coordinates x, y of the plate middle surface and the time t, and D is the flexural rigidity of the plate defined by:

$$D = \frac{Eh^3}{12\,(1-\nu^2)}$$

where E is Young's modulus, h is the plate thickness, ν in Poisson's ratio, and ρ is mass density per unit middle surface area of the plate. Equation (I-1) holds only for small lateral motions of the plate (less than approximately half the plate thickness) and neglects transverse shear and rotatory inertia.

If we introduce the Laplacian Operator ∇^2 into Equation (I-1), it will simplify to:

$$D\nabla^4 w + \rho\frac{\partial^2 w}{\partial t^2} = 0 \qquad (I\text{-}2)$$

Here $\nabla^4 = \nabla^2 \cdot \nabla^2$ and $\nabla^2 = \frac{\partial^2}{\partial x^2} + \frac{\partial^2}{\partial y^2}$

Using the method of separation of variables to solve Equation (I-2), we assume that $w(x,y,t) = G(t) \cdot F(x,y)$ (I-3)

If we substitute Equation (I-3) into Equation (I-2), we have:

$$\frac{D}{\rho} G(t)\,\nabla^4 F(x,y) + F(x,y)\frac{\partial^2 G(t)}{\partial t^2} = 0 \qquad (I\text{-}4)$$

Then, dividing Equation (I-4) through by $G(t) \cdot F(x,y)$ one finds:

$$\frac{D}{\rho} \frac{\nabla^4 F(x,y)}{F(x,y)} = - \frac{\partial^2 G(t)}{\partial t^2} / G(t) \qquad \text{(I-5)}$$

The left member of Equation (I-5) is clearly independent of t, and the right-hand side is independent of x and y. Thus, each side of Equation (I-5) must be a constant, say K^2, and we can write:

$$\frac{D}{\rho} \frac{\nabla^4 F(x,y)}{F(x,y)} = - \frac{d^2 G(t)/dt^2}{G(t)} = K^2 \qquad \text{(I-6)}$$

Thus, the original partial differential equation has been reduced to two equations

$$\nabla^4 F(x,y) - \frac{\rho}{D} K^2 F(x,y) = 0 \qquad \text{(I-7)}$$

and

$$\frac{d^2 G(t)}{dt^2} + K^2 G(t) = 0 \qquad \text{(I-8)}$$

The solution of the ordinary differential Equation (I-8) is:

$$G(t) = \overline{A} \cos(Kt) + \overline{B} \sin(Kt) \qquad \text{(I-9)}$$

where $\overline{A}$ and $\overline{B}$ are constants, and can be determined from initial conditions.

To solve Equation (I-7), one uses the method of separation of variables again. Assume:

$$F(x,y) = U(y) \cdot \sin(mx + \alpha) \qquad \text{(I-10)}$$

Substitution of Equation (I-10) into Equation (I-7) yields

$$\frac{d^4 U(y)}{dy^4} - 2m^2 \frac{d^2 U(y)}{dy^2} + (m^4 - K^2 \frac{\rho}{D}) U(y) = 0 \qquad \text{(I-11)}$$

which is an ordinary differential equation. The solution of (I-11) leads to three different cases, as follows:

$$U(y) = \begin{cases} e^{-\bar{E}y} & \text{if } m^2 > \sqrt{K^2\frac{\rho}{D}} \\ 1 & \text{if } m^2 = \sqrt{K^2\frac{\rho}{D}} \\ \cos(Ly) & \text{if } m^2 < \sqrt{K^2\frac{\rho}{D}} \end{cases} \qquad \text{(I-12)}$$

where

$$\bar{E} = \left[m^2 - \sqrt{K^2\frac{\rho}{D}}\right]^{\frac{1}{2}}$$

$$L = \left[\sqrt{K^2\frac{\rho}{D}} - m^2\right]^{\frac{1}{2}} \qquad \text{(I-13)}$$

Thus, the time-dependent, free, undamped vibrations of a thin, elastic plate are characterized by the lateral response $w(x,y,t)$ given by (I-3) where $G(t)$ is given by (I-9) and $F(x,y)$ is found from (I-10) with $U(y)$ given as one or the other of the three cases discussed.

The Edge-Function method involves the association of a different system of coordinate axes with each edge of the plate. Let us consider a rectangular coordinate system x,y as shown in Figure 1. With respect to this system, let the vertices P_1, P_2, ... P_i of the polygonal plate have coordinates (x_1, y_1), (x_2, y_2)---(x_i, y_i)---respectively. Each point P_i is chosen as the origin of a rectangular coordinate system $(\bar{x}_i, \bar{y}_i)$, the $\bar{x}_i$ axis of which makes an angle θ_i with the positive direction of the x-axis as shown below. This axis will ultimately be chosen to coincide with an edge of the plate.

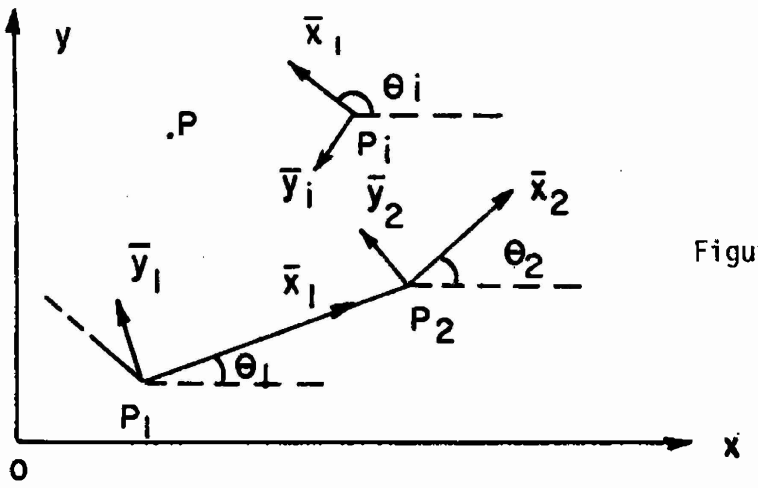

Figure 1

If a point P(x,y) in the (x,y) coordinate system has coordinates $\bar{x}_1$, $\bar{y}_1$, with respect to the ($\bar{x}_1$, $\bar{y}_1$) coordinate system, the relation between (x,y) and ($\bar{x}_1$, $\bar{y}_1$) is:

$$\begin{aligned} \bar{x} &= (x - x_1)\cos\theta_1 + (y - y_1)\sin\theta_1 \\ \bar{y} &= -(x - x_1)\sin\theta_1 + (y - y_1)\cos\theta_1 \end{aligned} \qquad \text{(I-14)}$$

as is evident from Figure 2

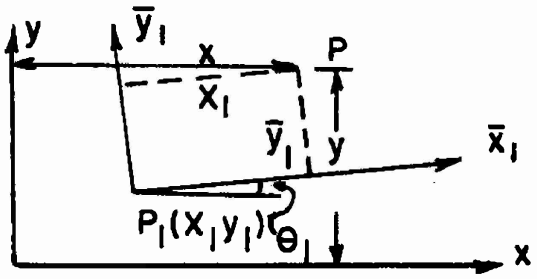

Figure 2

Analogous geometric relations may be found for the coordinates of point P is some ($\bar{x}_j$, $\bar{y}_j$) coordinate system in terms of its coordinates in the ($\bar{x}_i$, $\bar{y}_i$) system. Likewise, the partial differential relations between the (x,y) and the $\bar{x}_j$, $\bar{y}_j$) coordinate systems can be derived from the chain rule. For example, we have:

$$\frac{\partial}{\partial x} = \cos\theta_j \frac{\partial}{\partial \bar{x}_j} - \sin\theta_j \frac{\partial}{\partial \bar{y}_j}$$

$$\frac{\partial}{\partial y} = \sin\theta_j \frac{\partial}{\partial \bar{x}_j} + \cos\theta_j \frac{\partial}{\partial \bar{y}_j} \qquad \text{(I-15)}$$

The relationships between the various second derivatives are found to be:

$$\frac{\partial^2}{\partial x^2} = \cos^2\theta_j \frac{\partial^2}{\partial \bar{x}_j^2} - 2\sin\theta_j \cos\theta_j \frac{\partial^2}{\partial \bar{x}_j \partial \bar{y}_j} + \sin^2\theta_j \frac{\partial^2}{\partial \bar{y}_j^2}$$

$$\frac{\partial^2}{\partial y^2} = \sin^2\theta_j \frac{\partial^2}{\partial \bar{x}_j^2} - 2\sin\theta_j \cos\theta_j \frac{\partial^2}{\partial \bar{x}_j \partial \bar{y}_j} + \cos^2\theta_j \frac{\partial^2}{\partial \bar{y}_j^2}$$

$$\frac{\partial^2}{\partial x \partial y} = \left(\frac{\partial^2}{\partial \bar{x}_j^2} - \frac{\partial^2}{\partial \bar{y}_j^2}\right) \sin\theta_j \cos\theta_j + (\cos^2\theta_j - \sin^2\theta_j) \frac{\partial^2}{\partial \bar{x}_j \partial \bar{y}_j} \qquad \text{(I-16)}$$

Comparable relations exist for the various necessary third and fourth derivatives.

The Edge-Function Method

Consider a thin elastic plate having n straight sides of lengths $a_1, a_2, ---, a_n$. A right-hand Cartesian coordinate system in the plane of the plate is shown in Figure (3). The sides of the plate make angles $\theta_1, \theta_2, \theta_3, ---\theta_n$ with the x-axis.

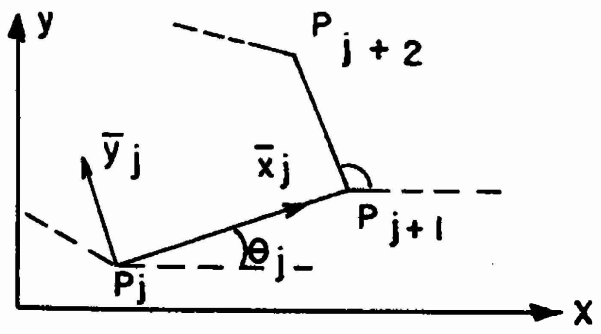

Figure 3

The equation of undamped motion of this plate was given as Equation (I-1) with respect to the (x,y) coordinate system:

$$\frac{\partial^4 w}{\partial x^4} + 2\frac{\partial^4 w}{\partial x^2 \partial y^2} + \frac{\partial^4 w}{\partial y^4} + \frac{\rho}{D}\frac{\partial^2 w}{\partial t^2} = 0 \qquad \text{(I-17)}$$

Now, if the vertex P_j of the plate is taken as an origin and side $P_j P_{j+1}$ is taken to coincide with the positive $\bar{x}_j$-axis and a $\bar{y}_j$ axis is selected which is normal to $\bar{x}_j$ and directed toward the interior of the plate, then a new coordinate system $(\bar{x}_j, \bar{y}_j)$ is obtained. Since the biharmonic operator is invariant under rotation and translation of axes, one immediately has:

$$\frac{\partial^4}{\partial x^4} + 2\frac{\partial^4}{\partial x^2 \partial y^2} + \frac{\partial^4}{\partial y^4} = \frac{\partial^4}{\partial \bar{x}_j^4} + 2\frac{\partial^4}{\partial \bar{x}_j^2 \partial \bar{y}_j^2} + \frac{\partial^4}{\partial \bar{y}_j^4} \qquad \text{(I-18)}$$

Using this concept, Equation (I-17) can be transformed as follows:

$$\frac{\partial^4 w}{\partial \bar{x}_j^4} + 2\frac{\partial^4 w}{\partial \bar{x}_j^2 \partial \bar{y}_j^2} + \frac{\partial^4 w}{\partial \bar{y}_j^4} + \frac{\rho}{D}\frac{\partial^2 w}{\partial t^2} = 0 \qquad \text{(I-19)}$$

After applying the method of separation of variables by letting $w(x, y, t) = F(x,y)G(t)$, a time-independent differential equation is obtained as follows:

$$\frac{\partial^4 F(x,y)}{\partial \bar{x}_j^4} + 2\frac{\partial^4 F(x,y)}{\partial \bar{x}_j^2 \partial \bar{y}_j^2} + \frac{\partial^4 F(x,y)}{\partial \bar{y}_j^4} - \frac{\rho}{D} K^2 F(x,y) = 0 \qquad \text{(I-20)}$$

or

$$\nabla^4 F(x,y) - \frac{\rho}{D} K^2 F(x,y) = 0$$

If the complementary solutions of Equation (I-19) are $F(\bar{x}_j, \bar{y}_j)$, $j = 1, 2, ---, n$, where $F(\bar{x}_j, \bar{y}_j)$ are related to the (x_j, y_j) coordinate system, then from the property of linear homogeneous differential equations, it follows that the superposition principle can be applied, hence the sum of those complementary solutions is also a solution of Equation (I-17), i.e.

$$F(x,y) = \sum_{j=1}^{n} F(\bar{x}_j, \bar{y}_j) \qquad \text{(I-21)}$$

Since $F(\bar{x}_j, \bar{y}_j)$ is a solution of Equation (I-17), and Equation (I-20) is identical to Equation (I-17), due to the invariance property, it can be said that $F(\bar{x}_j, \bar{y}_j)$ is a solution of Equation (I-20) or

$$\frac{\partial^4 F(\bar{x}_j, \bar{y}_j)}{\partial \bar{x}_j^4} + 2\frac{\partial^4 F(\bar{x}_j, \bar{y}_j)}{\partial \bar{x}_j^2 \partial \bar{y}_j^2} + \frac{\partial^4 F(\bar{x}_j, \bar{y}_j)}{\partial \bar{y}_j^4} - \frac{\rho}{D} K^2 F(\bar{x}_j, \bar{y}_j) = 0 \qquad \text{(I-22)}$$

The solution of Equation (I-22) is:

$$F(\bar{x}_j, \bar{y}_j) = \sum_{M=1}^{\infty} [A_{jM} e^{-H_j \bar{y}_j} + B_{jM} u_J(\bar{y}_j)] \sin(m_j \bar{x}_j + \alpha_j) \qquad \text{(I-23)}$$

where

$$u_j(\bar{y}_j) = \begin{cases} e^{-E_j\bar{y}_j} & \text{if} \quad m_j^2 > \sqrt{K^2\frac{\rho}{D}} \\ 1 & \text{if} \quad m_j^2 = \sqrt{K^2\frac{\rho}{D}} \\ \cos(L_j\bar{y}_j) & \text{if} \quad m_j < \sqrt{K^2\frac{\rho}{D}} \end{cases} \qquad \text{(I-24)}$$

and

$$H_j = \left[m_j^2 - \sqrt{K^2\frac{\rho}{D}}\right]^{\frac{1}{2}}; \qquad E_j = \left[m_j^2 - \sqrt{K^2\frac{\rho}{D}}\right]^{\frac{1}{2}} \qquad \text{(I-25)}$$

$L_j = \left[\sqrt{K^2\frac{\rho}{D}} - m_j^2\right]^{\frac{1}{2}}$, m_j is later found to be given by (5.6).

The required derivatives of (I-24) with respect to the $(\bar{x}_i, \bar{y}_i)$ coordinate system, where the origin is taken at the vertex P_i of the plate and the $\bar{x}_i$ axis coincides with the edge P_iP_i+1 are readily found through use of the chain rule.

Deflection, Normal Slope, Bending Moment, Twisting Moment, Kirchhoff Force

In discussing the free lateral vibrations of thin plates, the deflection, normal slope, bending moment, twisting moment and Kirchhoff force can be found as follows:

(a) Deflection

The deflection is defined as $w(x,y,t)$, where $w(x,y,t) = G(t) \cdot F(x,y)$ or

$$w(x,y,t) = G(t) \cdot \sum_{j=1}^{n} F(\bar{x}_j,\bar{y}_j) \qquad \text{(I-26)}$$

Substituting Equation (I-23) into Equation (I-26), it is seen that:

$$w(x,y,t) = G(t) \cdot \sum_{j=1}^{n} \sum_{M=1}^{\infty} [A_{jM}e^{-H_j\bar{y}_j} + B_{jM}u_j(\bar{y})]\sin(m_j\bar{x}_j + \alpha_j) \tag{I-27}$$

where $u_j(\bar{y}_j)$ is defined in Equation (I-24).

(b) Normal slope with respect to the x_i-axis:

The normal slope is defined as $\theta_i(x,y,t)$ where:

$$\theta_i(x,y,t) = \frac{\partial w(x,y,t)}{\partial \bar{y}_i}$$

or

$$\theta_i(x,y,t) = G(t) \cdot \frac{\partial F(x,y)}{\partial \bar{y}_i} \tag{I-28}$$

Thus:

$$\theta_i(x,y,t) = G(t) \cdot \sum_{j=1}^{n} \sum_{M=1}^{\infty} [A_{jM}\{m_j \sin\theta_{ij}\cos(m_j\bar{x}_j + \alpha_j) -$$

$$H_j\cos\theta_{ij}(\sin(m_jx_j + \alpha_j)\} \cdot e^{-H_j\bar{y}_j} + B_{jM}\bar{u}_j(\bar{x}_j\bar{y}_j)]$$

(c) Bending Moment with Respect to the x_j-axis:

The bending moment is defined as $M_{y_i}(x,y,t)$ where

$$M_{y_i}(x,y,t) = D\left(\frac{\partial^2 w(x,y,t)}{\partial \bar{y}_i^2} + \nu\frac{\partial^2 w(x,y,t)}{\partial \bar{x}_i^2}\right)$$

or

$$M_{y_i}(x,y,t) = -DG(t)\left(\frac{\partial^2 F(x,y)}{\partial \bar{y}_i^2} + \nu\frac{\partial^2 F(x,y)}{\partial \bar{x}_i^2}\right)$$

$$M_{y_i}(x,y,t) = + DC(t) \sum_{j=1}^{n} [A_{jM}\{m_j^2(\sin^2\theta_{ij} + \nu\cos\theta_{ij})\sin(m_j x_i + \alpha_j)$$

$$+ 2(1-\nu)H_j m_j \sin\theta_{ij}\cos\theta_{ij}\cos(m_j\bar{x}_j+\alpha_j) - H_j^2(\cos^2\theta_{ij}+\nu\sin^2\theta_{ij}) \cdot$$

$$\sin(m_j\bar{x}_j+\alpha_j)\} e^{-H_j\bar{y}_j} + B_{jM}\bar{\bar{u}}_j(\bar{x}_j,\bar{y}_j)] \qquad \text{(I-29)}$$

where U_j are functions of m_j, θ_{ij}, α_j, E_j, $\bar{x}_j$ and $\bar{y}_j$. In an analogous manner expressions are found for the twisting moment and Kirchhoff force, dentoed by R. A more general form is obtained if Q_{is} is taken to represent these quantities where

$$Q_{i1} = w_i,\ Q_{i2} = \theta_i,\ Q_{i3} = M_{yi},\ Q_{i4} = M_{x_i y_i} \text{ and } Q_{i5} = R.$$

Then one has

$$Q_{is}(\bar{P}_i) = G(t) \sum_{j=1}^{n} \sum_{M=1}^{\infty} [A_{jM}V_{jM}^{S}(\bar{x}_j,\bar{y}_j)+B_{jM}U_{jM}^{S}(\bar{x}_j,\bar{y}_j)] \qquad \text{(I-30)}$$

where V_{jM}^{S} and U_{jM}^{S} are functions of m_j, θ_{ij}, α_j, $\bar{x}_j$, and $\bar{y}_j$, and are given in complete detail in [7].

Boundary Conditions:

(a) Simply supported edge: If the edge of a plate is simply supported, the lateral deflection along this edge is zero, and there is no bending moment normal to this edge. Assuming that the simply supported edge is the i-th side of the plate, the boundary conditions there are:

$$\begin{aligned} &(1) \quad w(x,y,t) = 0 \qquad \text{at } \bar{y}_i = 0 \\ &(2) \quad M_{y_i}(x,y,t) = 0 \qquad \text{at } \bar{y}_i = 0 \end{aligned} \qquad \text{(I-31)}$$

(b) Clamped edge: If the edge of a plate is clamped, the deflection along this edge is zero, and the normal slope of this edge is also zero. If the i-th edge is the clamped one, then the boundary conditions there are:

$$\begin{aligned} &(1) \quad w(x,y,t) = 0 \qquad \text{at} \quad \bar{y}_i = 0 \\ &(2) \quad \theta_i(x,y,t) = 0 \qquad \text{at} \quad y_i = 0 \end{aligned} \tag{I-32}$$

(c) Free Edge:

$$\begin{aligned} &(1) \quad M_{y_i}(x,y,t) = 0 \qquad \text{at} \quad \bar{y}_i = 0 \\ &(2) \quad R(x,y,t) = 0 \qquad \text{at} \quad y_i = 0 \end{aligned} \tag{I-33}$$

where

$$R(x,y,t) = \left[\frac{\partial^3 W(x,y,t)}{\partial \bar{y}_i^3} + (2-\nu)\frac{\partial^3 W(x,y,t)}{\partial \bar{x}_i^2 \partial \bar{y}_i}\right]$$

which is sometimes termed the induced shear. The boundary conditions usually require that a suitable pair of the general Equations (I-30) be specified on each side of the plate. Physically, this means that two of the functions representing the deflection, the normal slope, the bending moment or the induced shear be defined on that edge. Let $\bar{P}_i$ be any point $(\bar{x}_i, 0)$ on the i-th edge and $Q_{is}(P_i)$ be one of the functions specified on that side. Accordingly, any boundary condition along the i-th edge is:

$$Q_{is}(\bar{P}_i) = G(t) \sum_{j=1}^{n} \sum_{M=1}^{\infty} (A_{jM} V_{jM}^s(\bar{P}_i) + B_{jM} U_{jM}^s(\bar{P}_i)] \tag{I-34}$$

where s assumes any one of the values 1, 2, 3, 4, or 5. Dividing by G(t) we have

$$\frac{Q_{is}(\bar{P}_i)}{G(t)} - \sum_{j=1}^{n} \sum_{M=1}^{\infty} [A_{jM} V_{jM}^s(\bar{P}_i) + B_{jM} U_{jM}^s(\bar{P}_i)]$$

$$\sum_{M=1} [A_{iM}V^S_{iM}(\bar{P}_i) + B_{iM}U^S_{iM}(\bar{P}_i)] = g(\bar{x}_i) \qquad \text{(I-35)}$$

The identity (I-35) is valid along the i-th edge, and must be satisfied for all $\bar{x}_i$ in the range $(0, a_i)$. Expanding $g(x_i)$ in a Fourier sine series, we have:

$$g(\bar{x}_i) = \sum_{M=1}^{\infty} C_M \sin(\frac{M\pi}{a} \bar{x}_i) = \sum_{M=1}^{\infty} [A_{iM}V^S_{iM}(\bar{P}_i) + B_{iM}U^S_{iM}(\bar{P}_i)] \qquad \text{(I-36)}$$

If we now multiply both sides of (I-35) by $\sin(\frac{N\pi}{a_i} \bar{x}_i)$, where N is any fixed positive integer) and integrate from 0 to a_i we are led to a system of an infinite number of equations for the values N=1, 2, 3,.....∞. These equations must, of course, be truncated after a finite number of harmonics, say M = L terms. Then the total number of unknowns A_{jM} and B_{jM} in Equation (I-34) is given by:

$$\text{Total unknowns} = 2 \times (\text{number of sides of plate}) \times L \qquad \text{(I-37)}$$

For the determination of these unknown constants, one requires 2 x (number of sides of plate) x L simultaneous equations. In the usual plate problem, there are two specified boundary conditions along each edge, thus the total number of specified conditions is 2 x (number of sides of plate). If the number N is $\bar{L}$ on every edge, then the total number of equations is:

$$\text{Total equations} = 2 \times (\text{number of sides of plate}) \times \bar{L} \qquad \text{(I-38)}$$

Comparing Equations (I-37) and (I-38), one observes that the number N of harmonic equations must equal the number of terms in the summation in M, i.e. it is required that $\bar{L} = L$. Solution of this set of equations yields the plate natural frequencies as well as relative amplitudes of free vibration in each mode.

It should be noted that when a plate has a free corner, or if the plate is skewed, additional functions are required. These are termed Fractional-Edge-Functions and are found from (I-36) by taking M as a fractional number and α_j to be non-zero. The fractional value is essentially determined by trial-and-error so as to minimize boundary residuals so as to best satisfy boundary conditions. These Fractional-Edge-Functions are added to the Edge-Function series (I-34) in the positions M = L+1 and L+2 where L is the truncation value.

Numerical Results

The first six natural frequencies for a square plate clamped on all four sides as obtained by the present method (using various numbers of harmonics from L = 2 to L = 6) are listed in Table 1. Also presented there are the results of S. Tomotika [8], D. Young [9], and S. Iguchi [10] for the same problem. The frequency parameter is $\lambda = K_a^2 \sqrt{\rho/D}$ where K is defined in (I-6).

TABLE 1

Source	Mode and λ					
	1	2	3	4	5	6
Tomotika [8]	35.99	--	--	--	--	--
Young [9]	35.99	73.41	108.27	131.64	132.25	165.15
Iguchi [10]	--	73.40	108.22	--	132.18	164.99
L = 2	35.572	72.80	107.08	--	130.28	167.78
L = 3	35.968	73.19	107.08	131.55	131.79	163.60
L = 4	35.970	73.35	108.12	131.55	131.79	164.25
L = 5	35.983	73.38	108.12	131.58	132.16	164.85
L = 6	35.984	73.39	108.20	131.59	132.16	164.93

It is interesting to note that the use of L = 6 involves only about 20 seconds of running time on a CDC 3600 computer to yield the first six frequencies indicated in Table 1. The values of deflections, slopes, moments, etc. at any point of the plate may now be readily found from the appropriate governing equations. There relative values are obtained by assigning to a specified point in the plate the parameter value unity, then comparing the values at other points to this unit value. To give an indication of the accuracy of the frequencies tabulated in Table 1, the R.M.S. values of the residual normal slopes along each of the four edges of the clamped square plate when vibrating in its first mode are indicated in Table 2.

TABLE 2

Boundary residual of normal slopes corresponding to the first mode of a square plate clamped on all sides.

No. of Harmonics	Boundary of the Plate			
	AB	BC	CD	DA
2	0.0914	0.0914	0.0914	0.0914
3	0.0131	0.0131	0.0131	0.0131
4	0.0131	0.0131	0.0130	0.0131
5	0.0033	0.0033	0.0033	0.0033
6	0.0032	0.0032	0.0032	0.0033

The first two natural frequencies of a square cantilever plate as illustrated in Figure 4 as determined by the present technique, as well as found by D. Young [9] using an energy approach are tabulated in Table 3.

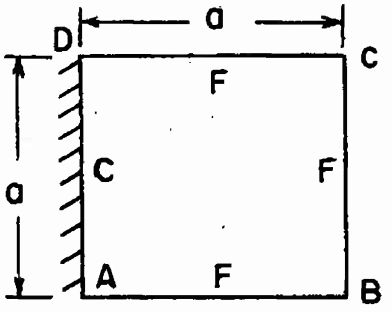

Figure 4

TABLE 3

SOURCE OF DATA	FREQUENCY PARAMETER λ	
	λ_1	λ_2
Young [9]	3.49	8.55
Edge-Functions	3.295	8.564

The R.M.S. values of a support deflection and free edge residual bending moment along DA are indicated in Table 4.

TABLE 4

	No. of Harmonics	
	L = 5	L = 7
Deflections along DA	0.0058	0.0022
Bending moments along AB	0.1533	0.0672
Bending moments along BC	0.0219	0.0121

Results for other cases such as square plates simply supported on all sides, rectangular plates simply supported on all sides, square and rectangular plates with two opposite edges simply supported and the other two edges clamped, square plates with three edges clamped and the fourth edge simply supported, rectangular plates with two adjacent edges simply supported and the other edges clamped, parallelogram plates simply supported on all sides and a rectangular cantilever plate are given in [7].

Conclusions

It has been found that the Edge-Function method is well-suited to determination of natural frequencies and associated mode shapes of thin elastic plates undergoing free vibration. For those cases where other methods have been used by previous investigators to determine these quantities, the Edge-Function method yielded results in excellent agreement with existing analytical results as well as experimental values when those were available.

The use of Edge-Functions for investigation of natural frequencies and mode shapes of thin plates yeilds an additional bonus not ordinarily found in other approximate methods, namely rapid determination of how well the specified boundary conditions have been satisfied. This is done by digital evaluation of significant structural parameters along the boundary, say deflection and slope for a clamped edge, which should, of course, vanish identically, but the small residuals corresponding to each of these parameters are routinely printed out be the computer. For a simply supported edge, the small residual deflections and bending moments at a number of points along the edge are routinely determined. Thus, only one may readily ascertain exactly how well the specified boundary conditions have been satisfied along all boundaries of the plate.

CHAPTER II

VIBRATIONS OF THIN ELASTIC SHELLS

Introduction

The objective of the present investigation is to present a new generalized approximate approach to the problem of the free vibrations of thin, elastic shallow shells. The technique is applicable to shell structures having an arbitrary polygonal contour in the base plane and arbitrary boundary conditions along this contour. The method extends the Edge-Function technique to the problem of shallow shell vibrations and permits rapid determination of natural frequencies and associated mode shapes with only modest amounts of computer effort. Further, the method permits evaluation of the errors involved in this approximate approach by indicating boundary residuals along each straight boundary of the base of the shell. The specific example of a shallow spherical shell is investigated in detail.

Fundamental Equations

The basic differential equations employed in this work to describe the behavior of a thin elastic shell in the absence of applied loads are those derived in Kraus [11]. The system of equations reduces to two simultaneous differential equations for the normal deflection w and the stress function ϕ of the form:

$$D\nabla^2\nabla^2 w + \nabla_k^2\phi = -\rho h \frac{\partial^2 w}{\partial t^2} \qquad \text{(II-1)}$$

$$\frac{1}{Eh}\nabla^2\nabla^2\phi - \nabla_k^2 w = 0 \qquad \text{(II-2)}$$

Where ∇^2 is the Laplace operator, k_x and k_y are curvatures in the x and y directions respectively, $\nabla_k^2 = k_y \frac{\partial^2}{\partial x^2} + k_x \frac{\partial^2}{\partial y^2}$, E represents Young's modulus, h the shell thickness, ν is Poisson's ratio, ρ the shell density, t denotes time, and $D = Eh^3/12(1-\nu^2)$. Normal and shear stress resultants as well as bending and twisting moments may be expressed in terms of w and ϕ as indicated in [11]. The tangential displacements u, v along the x and y axes respectively may be expressed in terms of w and ϕ from relations presented in [4]. For example, the first of these relations is:

$$\frac{\partial u}{\partial x} + k_x w = \frac{1}{Eh}\left(\frac{\partial^2 \phi}{\partial y^2} - \nu \frac{\partial^2 \phi}{\partial x^2}\right) \qquad \text{(II-3)}$$

Let us consider the case of a shallow spherical shell for which $k_x = k_y = k_y = k = 1/R$ where R is the radius of curvature of the shell middle surface. If both w and ϕ exhibit a harmonic dependence on time, i.e. if

$$w = W(x,y)\ \sin\omega t \qquad \text{(II-4)}$$

$$\phi = \phi(x,y)\ \sin\omega t \qquad \text{(II-5)}$$

then Equation (1) and (2) reduce to

$$D\nabla^4 W + k\nabla^2 \phi = \rho h \omega^2 W \qquad \text{(II-6)}$$

$$\frac{1}{Eh}\nabla^4 \phi - k\nabla^2 W = 0 \qquad \text{(II-7)}$$

where is the natural circular frequency of free vibration. It is possible to uncouple (II-6) and (II-7) into the form

$$\nabla^6 W - p^4 \nabla^2 W = 0 \qquad \text{(II-8)}$$

$$\nabla^8 \phi - p^4 \nabla^4 \phi = 0 \qquad \text{(II-9)}$$

where

$$p^4 = \frac{h}{D}(\rho\omega^2 - Ek^2) \qquad \text{(II-10)}$$

Since there are four conditions to be specified on each edge of the polygonal boundary the solutions for w and ϕ must contain four arbitrary constants.

For convenience, let us set

$$\psi = \nabla^4 W - p^4 W \qquad \text{(II-11)}$$

Substitution of this relation into (8) leads to

$$\nabla^2 \psi = 0 \qquad \text{(II-12)}$$

Formulation of Solution

The projection of the shell onto the x-y plane is considered to be a two-dimensional convex simply-connected region R, the closed boundary B of R being a polygon of J sides. As in Figure 5, a set of rectangular Cartesian coordinate axes Oxy is chosen and the vertices and sides of

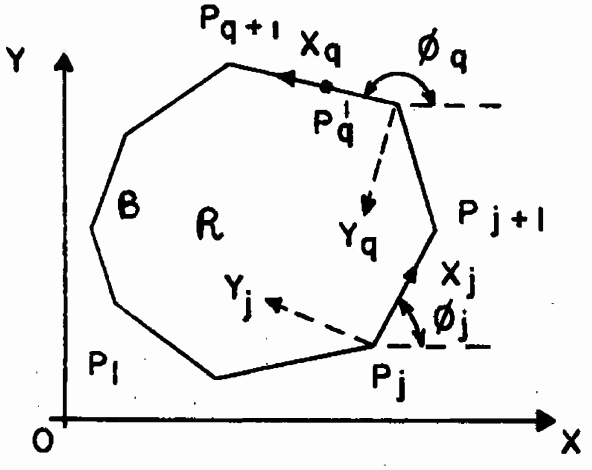

Figure 5

the polygon B are numbered 1 to J. The typical vertex P_j has coordinates (X_j, Y_j) in the Oxy reference frame and the typical side, the j^{th}, is P_jP_{j+1}, having length a_j and making an angle ϕ_j with the positive direction of the Ox axis. Associated with each side j is a set of edge-axes x_jy_j, having origin at P_j and directed along the (inward) normal to that side.

The fundamental series solution of Equation (II-12) in rectangular coordinates, derived using the separation of variables technique is:

$$\psi = \sum_{(m)} \{[A_m \sin(mx + \alpha_m) + B_m \cos(mx + \beta x)]e^{-my} + [C_m \sin(mx + \alpha_m) + D_m \cos(mx + \beta x)]e^{+my}\} \qquad \text{(II-13)}$$

where m, A_m, B_m, C_m, and D_m are as yet undetermined constants. The phase shifts α_m and β_m, although unnecessary here, are included for sake of generality later. Since the Laplacian operator ∇^2 is invariant under transformations which produce translation and rotation of axes, it follows that

$$\frac{\partial^2 \psi}{\partial x_j^2} + \frac{\partial^2 \psi}{\partial y_j^2} = 0 \qquad \text{(II-14)}$$

The solution of this equation will then take the form

$$\psi = \sum_{(m_j)} \{[A_m^j \sin(m_j x_j + \alpha_m) + B_m^j \cos(m_j x_j + \beta_m)]e^{-m_j y_j} + [C_m^j \sin(m_j x_j + \alpha_M) + D_m^j \cos(m_j x_j + \beta_m)]e^{+m_j y_j} \qquad \text{(II-15)}$$

in terms of the coordinates (x_jy_j) of a point referred to the j^{th} system of axes. Subscripts and superscripts j have been added to m and the constants A_m, B_m, C_m, and D_m to indicate association with the j^{th} side

of the boundary B. Clearly, similar expressions arise for solutions associated with each of the J sides of the polygon and all such solutions may be superposed, the governing differential equation being linear. Thus, a general solution may be put in the form

$$\psi = \sum_{j=1}^{J} \sum_{(m_j)} \{[A_m^j \sin(m_j x_j + \alpha_m) + B_m^j \cos(m_j x_j + \beta_m)]e^{-m_j y_j}$$

$$+ [C_m^j \sin(m_j x_j + \alpha_m) + D_m^j \cos(m_j x_j + \beta_m)]e^{m_j y_j}\} \qquad \text{(II-16)}$$

Analogous to the solution for a simple rectangular region, the constants m_j in (II-16) are chosen so that

$$m_j = 2M\pi/a_j \qquad \text{(II-17)}$$

for M a non-negative integer, in order to facilitate generation of the boundary condition equations later. Obviously the function ψ contributes to the determination fo the displacement components and stress couples. Thus, in general, in formulating the boundary conditions for the typical, j^{th}, side, the coefficients in (II-16) associated with the j^{th} side can be made implicitly dependent on the relevant boundary conditions. In the general solution at any point within the region R, the displacement components and stress resultants will be composed of contributions from each side of B, each contribution being dependent on the boundary conditions imposed on that particular side. Thus, invoking St. Venant's principle, it is physically desirable that such contributions decay with increasing distance from the corresponding side. So, in II-16), the coefficients C_m^j and D_m^j are set equal to zero. Consequently, ψ is chosen to be:

$$\psi = \sum_{j=1}^{J} \sum_{M} [A_{1M}^{j} \sin(m_j x_j + \alpha_m) + B_{1M}^{j} \cos(m_j x_j + \beta_m)] e^{-m_j y_j} \qquad \text{(II-18)}$$

in which m_j is defined in (II-17).

Each of the fundamental terms $e^{-m_j y_j} \sin(m_j x_j + \alpha_m)$ and $e^{-m_j y_j} \cos(m_j x_j + \beta_m)$ in ψ now possesses the advantageous properties of being directly associated with the j-th side of the boundary and of decaying in contribution to the overall solution with increasing distance y_j into the region from that side. Such functions, similar both in form and notation to those employed by Tai and Nash [7], are termed edge-functions. Comparable expressions for may be written but are omitted for brevity. If one substitutes (II-18) into (II-11) and also carries out a comparable procedure for ϕ, one finally obtains

$$W = \sum_{j=1}^{J} \sum_{M} \{[-\frac{1}{p^4} A_{1M}^{j} e^{-m_j y_j} + A_{3M}^{j} e^{-(m_j^2 + p^2)^{1/2} y_j} +$$

$$A_{4M}^{j} e^{-(m_j^2 - p^2)^{1/2} y_j}] \sin(m_j x_j + \alpha_m) +$$

$$[-\frac{1}{p^4} B_{1M}^{j} e^{-m_j y_j} + B_{3M}^{j} e^{-(m_j^2 + p^2)^{1/2} y_j} +$$

$$B_{4M}^{j} e^{-(m_j^2 - p^2)^{1/2} y_j}] \cos(m_j x_j + \beta_m)\} \qquad \text{(II-19)}$$

and

$$\phi = \sum_{j=1}^{J} \sum_{M} \{[-\frac{1}{p^4}(A_{2M}^{j} - \frac{\rho h \omega^2}{2 m_j^2 k} m_j y_j A_{1M}^{j}) e^{-m_j y_j} +$$

$$\frac{Ehk}{p^4}(A_{3M}^{j} e^{-(m_j^2 + p^2)^{1/2} y_j} - A_{4M}^{j} e^{-(m_j^2 - p^2)^{1/2} y_j})]$$

$$\cdot \sin(m_j x_j + \alpha_m) + [-\frac{1}{p^4}(B_{2M}^{j} - \frac{\rho h \omega^2}{2 m_j^2 k} m_j y_j B_{1M}^{j})$$

$$\cdot e^{-m_j y_j} + \frac{Ehk}{p^2}(B_{3M}^{j} e^{-(m_j^2 + p^2)^{1/2} y_j} -$$

$$B_{4M}^{j} e^{-(m_j^2 - p^2)^{1/2} y_j})] \cos(m_j x_j + \beta_m)\} \qquad \text{(II-20)}$$

The expression for the transverse deflection (II-19) reduces in the case of zero curvature, $k = 0$, to the corresponding expression obtained by Tai and Nash [7] for the transverse deflection of a thin flat plate.

Shell boundary conditions are expressed in terms of various combinations of the parameters W, Φ, the in-plane displacements u_q and v_q along and perpendicular to the q-th side of the boundary, the rotation β about the tangent to the q-th side, the rotation β_q' about the normal to the q-th side, the in-plane stress resultant N_q, the bending moment M_q about the q-th side, the twisting moment M_{nt}^q about that same side, the Kirchhoff effective shearing stress resultants T_q and V_q, and the in-plane shearing stress resultant N_{nt}^q, all associated with the q-th edge. Expressions for each of these twelve parameters are derivable in terms of the coefficients A_{iM}^j and B_{iM}^j but are omitted for brevity. However, it is convenient to symbolize these boundary functions in the form

$$\Lambda_t$$

where t is an integer ranging from 1 to 12 for the above parameters W, Φ, u_q, etc. respectively. Further, let us introduce the function $\Lambda_t E_M^j$ to denote the edge-function contribution to Λ_t stemming from the j-th coordinate system and associated with the particular value M. In this case each of the above boundary functions may be written in the form

$$\Lambda_t = \sum_{j=1}^{J} \sum_{M} \Lambda_t E_M^j \qquad \text{(II-21)}$$

It is necessary to determine values for the frequency as well as the coefficients A_{iM}^j and B_{iM}^j so as to satisfy boundary conditions. Thus, boundary conditions require that four of the functions Λ_t be specified on each edge of the polygonal boundary. This is accomplished as follows.

If P'_q is any point $(x_q,0)$ on the q-th side of the boundary, as in Figure 1, the function $\Lambda_t(P'_q)$ is specified for four values of the parameter t t_q^1, t_q^2, t_q^3 and t_q^4, say. Consequently, equation (II-21) implies that

$$\Lambda_t(P'_q) = \sum_{j=1}^{J} \sum_{M} \Lambda_t E_M^j(P'_q)$$

$$t = t_q^1, t_q^2, t_q^3, t_q^4; \quad q = 1,2,\ldots,J \qquad \text{(II-22)}$$

In order to obtain identity equations for the coefficients A_{iM}^j and B_{iM}^j, it is noted that the series of terms

$$\sum_{(M)} \Lambda_t E_M^q(P'_q)$$

in the summation (II-22) does not contain negative exponential factors since $y_q = 0$, so that each term involves only x_q. Since the negative exponentials tend to diminish boundary influences this series of terms is dominant and consequently (II-22) may be written

$$\Lambda_t(P'_q) - \sum_{j=1}^{J} \sum_{M} \Lambda_t E_M^j(P'_q) = \sum_{M} \{ \sum_{i=1}^{4} (h_i A_{iM}^q + g_i B_{iM}^q)$$

$$\sin(m_q x_q + \alpha_m) + \sum_{i=1}^{4} (h_{i+r} A_{iM}^q + g_{i+4} B_{iM}^q)$$

$$\cos(m_q x_q + \beta_m)\} \qquad \text{(II-23)}$$

The dash in the summation $\sum'_{j=1}^{J}$, indicates that the term j = q is omitted. The factors h and g in (II-23) are independent of x_q and may readily be obtained from the expressions for $_tE_M^q$ by setting $y_q = 0$. Thus the left hand side of (II-23) is some function $H(x_q)$ of x_q and the identity can be satisfied provided that $H(x_q)$ can be expanded in the trigonometric form of the series on the right-hand side. On choosing

$$m_q = 2M\pi/a_q, \qquad M = 0,1,2,\ldots \qquad \text{(II-24)}$$

and

$$\alpha_m = \beta_m = 0 \qquad \text{(II-25)}$$

the right-hand side of (II-23) may be considered the Fourier series expansion of $H(x_q)$ in the range $[0,a_q]$.

Several methods of approximately satisfying the boundary identities (II-23) may be employed. Perhaps the most obvious is to multiply (II-23) by

$$\sin \frac{2N}{a_q} x_q dx_q$$

and integrate from 0 to a_q, then repeat using the cosine function. This leads to a set of equations of the form

$$G(x_q) = 0 \qquad \text{(II-26)}$$

which is actually an infinite set of equations in an infinite number of unknowns. It is of course necessary to truncate these equations at some level, say L_j, for each side j of the polygon.

Because the truncation of the harmonic series expansion of $G(x_q)$ at $N = L_q$ implies that the approximation

$$G(x_q) = \frac{1}{2}E_0 + \sum_{N=1}^{L_q} \left[E_N \cos \frac{2N\pi}{a_q} x_q + F_N \sin \frac{2N\pi}{a_q} x_q\right] \qquad \text{(II-27)}$$

is being used, another way to approximate $G(x_q)$ is to use trigonometric interpolation to fit a finite trigonometric series to $G(x_q)$ by a discrete least squares method. As is shown in [12], if a discrete Fourier series interpolation, based on discrete least squares fitting at $2k^*-1$ equidistant internal points in the interval $[0,a_q]$ is used in approximation (II-27), then

$$E_N = \frac{1}{k^*} \sum_{k=0}^{2k^*} w_k G(x_k) \cos \frac{2N\pi}{a_q} x_k \qquad N = 0,1,2,\ldots,L_q$$

$$F_N = \frac{1}{k^*} \sum_{k=1}^{2k^*-1} w_k G(x_k) \sin \frac{2N\pi}{a_q} x_k \qquad N = 1,2,\ldots,L_q \qquad \text{(II-28)}$$

where

$$x_k = ka_q/2k^* \tag{II-29}$$

and w_k are weight factors defined by

$$\begin{aligned} w_k &= 1/2: \qquad k = 0, \quad k = 2k^* \\ &= 1: \qquad 0 < k < 2k^* \end{aligned} \tag{II-30}$$

The expressions (II-28) for E_N and F_N may be set to zero thus generating the requisite set of simultaneous boundary equations. This interpolation method of setting up the simultaneous equations has the advantage, over the first method above, of requiring less computational time. Furthermore, it is found in practice that there is very little difference in accuracy between the results obtained from either method.

The set of equations arising from expression (II-27) in which the coefficients of the expansion must be set to zero, ensures that the boundary conditions (II-22) are satisfied at all points of the q-th side, $q = 1,2,\ldots,J$, except possibly at the vertices. If the boundary conditions are not automatically satisfied at the end points of each side of the polygon, they must be imposed at these points. Thus it is required to set to zero both the boundary function and its derivative along the relevant side, so that

$$G(x_q) = 0 \tag{II-31}$$

and

$$\frac{\partial}{\partial x_q} G(x_q) = 0 \tag{II-32}$$

for both ends $x_q = 0$ and $x_q = a_q$ of the interval and for each of the boundary functions corresponding to $t = t_q^1$, t_q^2, t_q^3, and t_q^4. The effect of these point equations, which are referred to as <u>vertex equations</u>, is not alone to ensure that the boundary conditions are satisfied at the end points of

the interval, but also to increase the rate of convergence of the Fourier series from order $1/M$ to at least order $1/M^3$. Such equations clearly give rise to the necessity of introducing additional unknowns in the basic solutions (II-19) and (II-20). Since, in general, there are four vertex equations arising for each boundary condition on each side, a total of sixteen additional unknowns associated with each side are required. These are provided by using fractional-edge-functions. The latter are edge functions of the types in expressions (II-19) and (II-20) within the summation signs. Whereas in the above harmonic edge-functions

$$m_q = 2M\pi/a_q, \qquad M = 0,1,\ldots,L_q, \quad \alpha_m = 0; \quad \beta_m = 0 \tag{II-33}$$

for the fractional-edge-functions new values of these parameters are defined, so that

$$m_q = 2V_M\pi/a_q; \quad \alpha_m \neq 0; \quad \beta_m \neq 0 \tag{II-34}$$

where V_M is non-integral. The sixteen requisite unknowns can be provided by including in the solution two fractional-edge-functions generated simply by choosing two different values for V_M. They may be incorporated in the general solution by adopting the convention that they correspond to $M = -1$ and $M = -2$ in the summations in (II-19) and (II-20). It may be noted that, in theory, the solution is independent of the choice of the vertex numbers V_M and of α_m and β_m for the fractional-edge-functions. However, in practice it is found that a judicious choice of values will increase the convergence of the truncated series solution.

It was found in [7] that the problem of free vibrations of flat plates could be successfully treated by use of a combination of edge functions and fractional edge functions. That is, the prescribed boundary conditions could be satisfied to the desired degree of accuracy. In the case of shell

vibrations this is not the case and it becomes necessary to employ not only the two types of functions used in plate analysis, but in addition a third type of function termed a shell polar function. This function contributes to the time-dependent deflections in the interior regions of the shell away from the boundaries, whereas the edge functions contribute largely in the immediate vicinity of the shell edges. The shell polar functions are of the form

$$\phi = \mathrm{Re}[EZ^{\lambda} + F\,\bar{Z}Z^{\lambda+1}]$$
$$W = \mathrm{RE}[F',\ Z^{\lambda}] \qquad \text{(II-35)}$$

where $z = x + iy$ (origin at any convenient interior point), $\bar{z}$ is the complex conjugate, E, F, and F' are complex constants, and λ is an integer. Details of the derivation and accompanying properties of these special functions are presented in the Appendix.

The shell polar functions are appended to the solutions to replace some (or possibly all) of the fractional edge functions. The selection of the ratio of fractional edge functions to shell polar functions is made on the basis of experience and judgment in use of this technique but with the requirement that boundary conditions be satisfied to the prescribed degree of accuracy. In the present investigation of a combination of half edge functions and half polar functions was found best for satisfying the prescribed boundary conditions.

Application of the boundary conditions leads to a system of homogeneous equations in the unknowns A^{j}_{iM} and B^{j}_{iM} of the form

$$\Sigma C_{ab}(\omega)A_b = 0, \qquad b = 1, 2 \qquad \text{(II-36)}$$

where A_b represents A^j_{iM} and B^j_{iM}. The C_{ab} are coefficients obtained from the interpolation method mentioned previously and are functions of the unknown frequency ω. The frequencies are found by setting the determinant of the system equal to zero, viz:

$$|C_{ab}(\omega)| = 0 \qquad \text{(II-37)}$$

Values of ω are determined by a suitable iteration method, such as the bisection procedure.

Numerical Results

Let us consider the free vibrations of a thin, elastic shallow spherical steel shell of square plan-form. The radius of curvature is 30.0 inches, the shell thickness 0.05 inches, the length of each side 12.0 inches (in plan-form), $E = 30 \times 10^6$ lb/in^2, Poisson's ratio = 0.3 and the material density is 0.732×10^{-3} lb-sec^2/in^4. Boundary conditions to be considered are (a) all sides simply supported, and (b) all sides clamped. Natural frequencies and associated mode shapes are desired. The natural frequencies are indicated by Equation (II-37) and a computer program for determination of these frequencies, associated mode shapes, and boundary residuals is available upon request from the authors [13].

For the case of simply supported edges, the first four natural frequencies are indicated below. Results are compared to those due to Vlasov [14] as well as Malkina [15]. The investigation [15] applies to the case of a spherical dome with circular plan-form but is employed here as an approximation by considering the greatest circular base to be inscribed in the square plan-form shell under consideration.

Frequency	1	2	3	4
Present Method				
L=1	6748.86	6759.30	6763.15	6829.48
L=7	6748.85	6759.30	6863.63	6795.35
Vlasov [14]	6749.51	6759.29		6827.35
Malkina [15]	6749.42		6762.31	

The computer program developed indicates the small residual bending moments along each of the sides of the shell. For example, for the first natural frequency if the peak bending moment at the mid-point of the shell is taken to be unity, the root-mean-square-boundary residual bending moment (for L=7) is found to be 0.37×10^{-2}. This same function for the fourth natural frequency is found to be 0.88×10^{-5}. Clearly these constitute very adequate satisfaction of boundary conditions.

For the case of a clamped edge spherical shell, the first four natural frequencies are indicated below, as well as those found by the Malkina method [15] again using the greatest inscribed circular base.

Frequency	1	2	3	4
Present Method				
L=1	6746.24	6794.72		
L=7	6746.24	6788.39	6992.20	7135.09
Malkina [15]	6746.24	6796.89	6998.91	

Again, the computer program displays the small residual deflections along the shell boundary. For example, for the first natural frequency the root-mean-square boundary deflection is 0199×10^{-3} (for L=3) and for the fourth natural frequency it is 0.75×10^{-5} (for L=3) compared

to peak mid-point deflection taken to be unity. Mode shapes are found by calculating the relative deflections of closely spaced points on the shell then connecting all zero-deflection points at a given frequency.

Conclusions

The present investigation has indicated that, for the geometry considered, the Edge Function Method is well-suited to determination of natural frequencies and associated mode shapes of thin elastic shallow shells undergoing free vibration. For the cases discussed through specific examples, the present analysis yielded results in excellent agreement with existing analytical results.

The computer program developed during the course of the present investigation is applicable to any spherical shell of n-sided plan-form. Further, the boundary conditions along each edge are completely arbitrary and may be different on the various edges without giving rise to complications in frequency determination.

The use of the present technique of analysis for determination of natural frequencies and mode shapes of thin elastic shells yields an additional bonus not originally found in other approximate methods, namely rapid determination of how well the specified boundary conditions have been satisfied. This is accomplished through digital evaluation of significant structural parameters along the boundary, say delfection and slope for a clamped edge which should, of course, vanish identically but the small residuals corresponding to each of these parameters are routinely printed out by the computer and root-mean-square values along any of the polygonal edges displayed. Thus, one may readily ascertain exactly how well the specified boundary conditions have been satisfied along all boundaries of the plate.

APPENDIX

SHELL POLAR FUNCTIONS

Equation (II-9) gives for

$$\nabla^4(\nabla^4 - p)\phi = 0 \tag{A-1}$$

one solution of which is

$$\nabla^4\phi = 0$$

from which, following O'Callaghan [12]

$$\phi = \mathrm{Re}[Ez^{\lambda} + F\bar{z}z^{\lambda+1}]; \quad z = x + iy \tag{A-2}$$

where E and F are complex constants and λ is arbitrary. Accordingly on substituting for $\nabla^4\phi$ in (7), we obtain

$$\nabla^2 W = 0 \tag{A-3}$$

and Equation (II-6) then gives

$$W = \frac{k}{\rho h\omega^2}\ \nabla^2\phi \tag{A-4}$$

On introducing the operators

$$\frac{\partial}{\partial x_q} = e^{i\phi_q}\frac{\partial}{\partial z} + e^{-i\phi_q}\frac{\partial}{\partial \bar{z}}$$

$$\frac{\partial}{\partial y_q} = ie^{i\phi_q}\frac{\partial}{\partial z} - ie^{i\phi_q}\frac{\partial}{\partial \bar{z}} \tag{A-5}$$

from which

$$\frac{\partial^2}{\partial x^2} + \frac{\partial^2}{\partial y^2} = 4\,\frac{\partial^2}{\partial z\partial \bar{z}}$$

and on operating with ∇^2 on (A-2) and substituting in (A-4), we obtain

$$W = \frac{4(\lambda+1)}{\rho hr\omega^2}\,\mathrm{Re}[Fz^{\lambda}] = \mathrm{Re}(F'z^{\lambda}] \tag{A-6}$$

where

$$F' = qF; \quad q = \frac{4(\lambda+1)}{\rho h r \omega^2} \tag{A-7}$$

To fit into the general polar form for the t^{th} derived function

$$Q_t = \mathrm{Re}[EAz^{\lambda^*} + F(B\bar{z}z^{\lambda^*+1} + Cz^{\lambda^*+2})] \tag{A-8}$$

where A, B, and C are complex functions of ϕ and λ, and where necessary will have a subscript t - A_t, B_t, C_t - to distinguish the different functions. Equation (A-6) for W then gives:

$$A = 0; \quad B = 0; \quad C = 2; \quad \lambda^* = \lambda-2 \tag{A-9}$$

Values of A, B, and C for each of the remaining eleven parameters ϕ, u_q, v_q, etc. are tabulated below.

Function	t	λ^*	A_t	B_t	C_t
W	1	$\lambda-2$	q	0	0
ϕ	2	λ	1	1	0
u_q	3	$\lambda-1$	$A_0e^{i\phi_q}$	$B_0e^{i\phi_q}$	$C_0e^{-i\phi_q}$
v_q	4	$\lambda-1$	iA_3	iB_3	$-iC_3$
β_q	5	$\lambda-1$	A_4/r	B_4/r	$C_4/r-i\ C_1e^{i\phi_q}/z^2$
N_q	6	$\lambda-2$	$(\lambda-1)e^{2i\phi_q}$	$(\lambda+1)e^{2i\phi_q}$	$2(\lambda+1)$
M_q	7	$\lambda-4$	0	0	$D^*\lambda(\lambda-1)e^{2i\phi_q}$
M_{nt}^q	8	$\lambda-4$	0	0	iC_7
T_q	9	$\lambda-2$	A_{12}	B_{12}	$C_{12}+C_8/rz^2$
V_q	10	$\lambda-5$	0	0	$(\lambda-2)^{i\phi_q}C_8/r$
β_q	11	$\lambda-1$	A_4/r	B_4/r	$C_4/r-\lambda e^{i\phi_q}\ C_1/z^2$
N_{nt}^q	12	$\lambda-2$	$-i\lambda(\lambda-1)e^{2i\phi_q}$	$-i\lambda\lambda'$	0

$$D^* = D(1-\nu)$$
$$\lambda' = (\lambda+1)e^{2i\phi_q}$$

CHAPTER III

RELIABILITY OF NONLINEAR STRUCTURES UNDER RANDOM EXCITATION

Introduction

The reliability of structures subject to random excitation has become a topic of increasing importance to designers. For example, flight vehicles are often subject to turbulence, random wind gusts, jet engine pressures, rocket exhausts, and other pressure fields that are random in nature. Actually, these are almost always nonstationary phenomena. However, because of the difficulties involved in analysis of nonstationary situations it is necessary to first consider the response of structures to stationary excitation, i.e. the statistical characteristics of the pressure fields are invariant under time shifts. The nonlinearity under consideration is geometric in nature, which characterizes large deflections of structural members. The present investigation is confined to the response of a single degree of freedom system.

In the present work the perturbation method [16] is used to deal with the nonlinear differential equations. Since this method has its limitations [17], we also use the Monte Carlo simulation method [18] to ascertain the range of validity of the perturbation results. Knowing the response, it is usually not difficult to determine significant system stresses. From this type of analysis together with considerations of first-crossing and fatigue [19] it is possible to predict the reliability of narrow-band type structures subject to stationary random excitation.

The Perturbation Method

If a nonlinear single-degree-freedom system is governed by the

equation:

$$\ddot{X}(t) + 2\omega_n \xi \dot{X}(t) + \omega_n^2 (X(t) + \mu X^3(t)) = f(t) \qquad \text{(III-1)}$$

where ξ is the damping ratio, ω_n the natural frequency of the corresponding linear system, μ a perturbation parameter which is dependent upon properties of structure, and $f(t)$ is a generalized force which is a stationary Gaussian random process with mean zero and the spectral density function $\phi(\omega)$.

We assume a solution of (III-1) in the form of a power series in μ:

$$X(t) = X_0(t) + \mu X_1(t) + \mu^2 X_2(t) + \ldots$$

For convenience, let

$$X = X_0 + X_1 + \mu^2 X_2 + \ldots \qquad \text{(III-2)}$$

If $E[\ ]$ denotes ensemble average, then

$$E(X\,X^*] = E[X_0 X_0^*] + \mu(E[X_0 X_1^*] + E[X_0^* X_1]) + \mu^2(E[X_0 X_2^*] + E[X_1 X_1^*] + E[X_0^* X_2] + \ldots \qquad \text{(III-3)}$$

where $X^* = X(t+\tau)$ and $E[X_0 X_0]$, $E[X_0 X_1^*]$, $E[X_0^* X_1]$,... are to be determined.

When (III-2) is inserted in (III-1), we get

$$(\ddot{X}_0 + \ddot{X}_1 + \mu^2 \ddot{X}_2 + \ldots) + 2\omega_n \xi (\dot{X}_0 + \mu \dot{X}_1 + \mu^2 \dot{X}_2 + \ldots) + \omega_n^2 [X_0 + \mu X_1 + \mu^2 X_2 + \ldots + \mu(X_0 + \mu X_1 + \ldots)^3] = f(t)$$

or

$$(\ddot{X}_0 + 2\omega_n \xi \dot{X}_0 + \omega_n^2 X_0) + \mu(\ddot{X}_1 + 2\omega_n \xi \dot{X}_1 + \omega_n^2 X_1 + \omega_n^2 X_0^3) + \mu^2(X_2 + 2\omega_n \xi \dot{X}_2 + \omega_n^2 X_2 + 3X_0^2 X_1 \omega_n^2) + \mu^3 (\ldots) + \ldots = f(t) \qquad \text{(III-4)}$$

The coefficient of each power of μ must separately vanish since (III-4) is to be satisfied identically in μ. Thus, we obtain a set of governing

equations for the X(t). The first of these represents the unperturbed system.

$$\ddot{X}_0 + 2\omega_n\xi\dot{X}_0 + \omega_n^2 X_0 = f(t)$$

$$\ddot{X}_1 + 2\omega_n\xi\dot{X}_1 + \omega_n^2 X_1 = -\omega_n^2 X_0^3$$

$$\ddot{X}_2 + 2\omega_n\xi\dot{X}_2 + \omega_n^2 X_2 = -3\omega_n^2 X_0^2 X_1 \qquad \text{(III-5)}$$

Because we treat the excitation f(t) as a stationary random process, the response is also a stationary random process after the transient period, and properties of the response can be deduced from that of the excitation. From random process analysis [20], we obtain the solution of (III-5) and also

$$E[X_0 X_0^*] = \int_{-\infty}^{\infty}\int_{-\infty}^{\infty} R_f(\tau + \theta_1 - \theta_2)\, h(\theta_1)h(\theta_2)d\theta_1 d\theta_2 \qquad \text{(III-6)}$$

$$E[X_0 X_1^*] = \int_{-\infty}^{\infty}\int_{-\infty}^{\infty} -\omega_n^2 E[f(t-\theta_1)X_0^3(t - \tau - \theta_2)]h(\theta_1)h(\theta_2)d\theta_1 d\theta_2 \qquad \text{(III-7)}$$

$$E(X_0^* X_1] = \int_{-\infty}^{\infty}\int_{-\infty}^{\infty} -\omega_n^2 E[f(t + \tau - \theta_1)X_0^3(t - \theta_2)]h(\theta_1)h(\theta_2)d\theta_1 d\theta_2 \qquad \text{(III-8)}$$

where R_f is the autocorrelation of f(t) and $h(\theta)$ is an impulse-response function.

To make the perturbation method more efficient, we have to simplify equations (III-6), (III-7), and (III-8). Since the autocorrelation function and power spectral density function as well as complex-frequency response $H(\omega)$ and unit-impulse response function $h(\theta)$ are related through the Fourier Integral, then (III-6) can be written as

$$E[X_0 X_0^*] = \int_{-\infty}^{\infty} \phi(\omega)|H(\omega)|^2 \exp(i\omega\tau)\, d\omega \qquad \text{(III-9)}$$

$$\sigma_{X_0}^2 = \int_{-\infty}^{\infty} \phi(\omega)|H(\omega)|^2\, d\omega \qquad \text{(III-9a)}$$

For (III-7), (III-8), we can apply the Gaussian property [17] and get the

final result:

$$E[X_0 X_1^*] = E[X_0^* X_1] = -3\omega_n^2 \sigma_{X_0}^2 \int_{-\infty}^{\infty} \phi(\omega)|H(\omega)|^2 H'(\omega)\exp(i\omega\tau)\, d\omega \quad \text{(III-10)}$$

When μ is not too large, for simplicity, we evaluate (III-3) to the first order of . Substituting (III-9) and (III-10) into (III-3)

$$E[X\, X^*] = \int_{-\infty}^{\infty} \phi(\omega)|H(\omega)|^2 \exp(i\omega\tau)\{1 - 6\mu\omega_n^2 \sigma_{X_0}^2 H'(\omega)\}\, d\omega \quad \text{(III-11)}$$

$$\sigma_X^2 = \int_{-\infty}^{\infty} \phi(\omega)|H(\omega)|^2 (1 - 6\mu\omega_n^2 \sigma_{X_0}^2 H'(\omega))\, d\omega \quad \text{(III-11a)}$$

where

$$H(\omega) = \frac{1}{\omega_n^2 - \omega^2 + 2i\xi\omega_n\omega}$$

$$H'(\omega) = \frac{\omega_n^2 - \omega^2}{(\omega_n^2 - \omega^2)^2 + (2\xi\omega_n\omega)^2}$$

Although it is very easy using the digital computer to calculate (III-9a) and (III-11a), the pitfall of this method lies in the fact that we cannot prove (III-2) is convergent and actually represents a solution of (III-1) within an acceptable error. Theoretically, this method is only for slightly nonlinear systems, i.e. μ is very small. However, this kind of knowledge is limited. With the purpose of broadening the applicability of this method, we take advantage of Monte Carlo simulation to solve (III-1) and compare the results with those from the perturbation method.

Monte Carlo Simulation

We have already known that the excitation f(t) is a stationary Gaussian random process with mean zero and the mean-square spectral density function $\phi(\omega)$. This process can be simulated [18] by the following series:

$$f_o(t) = \sigma_f \sqrt{\frac{2}{N}} \sum_{k=1}^{N} \cos(\omega_k t + \phi_k) \qquad \text{(III-12)}$$

with ϕ_k being uniformly distributed between 0 and 2π and independent of ϕ_j for $k \neq j$ and with ω_k being a random variable independent of ω_j for $k \neq j$ and of ϕ_j and distributed according to the density function:

$$g(\omega) = \frac{(\omega)}{\sigma_f^2} \qquad \text{(III-13)}$$

where

$$\sigma_f^2 = \int_{-\infty}^{\infty} \phi(\omega) d\omega \qquad \text{(III-13a)}$$

is the variance of the process f(t).

It is reasonable to simulate f(t) in this way because the simulated process $f_o(t)$ has the same autocorrelation function and spectral density function as f(t).

There are many basic methods for generating variates from the given probability distribution. The inverse transformation method seems the most convenient if it can be employed. We first obtain the cumulative distribution function $F_g(\omega)$ and set $F_g(\omega) = r$:

$$F_g(\omega) = \int_{-\infty}^{\omega} g(\omega')\, d\omega' = r \qquad \text{(III-14)}$$

Now, it is possible to find a particular ω_i corresponding to r_i by the inverse function of F_g if it can be obtained

$$\omega_i = F_g^{-1}(r_i) \qquad \text{(III-14a)}$$

where r, r_i are random numbers which are generated by different processes [21]. In case we cannot express in terms of $F_g^{-1}(\omega)$, we must either calculate a numberical approximation to F_g^{-1} or introduce another method instead of using (III-14a).

Once the generized force f(t) is simulated by (III-12) and (III-14a), (III-1) can be solved numerically. The accuracy of this approach is checked

against the exact solution obtained for the corresponding linear system. We use the Duhamel Integral equation [22] to solve (III-1) with $\mu = 0$:

$$X(t) = A(t)\sin(\omega_D t) - B(t)\cos(\omega_D t) \tag{III-15}$$

where

$$A(t) = \frac{1}{m\omega_D} \int_0^t f_o(t') \frac{e^{\xi\omega_n t'}}{e^{\xi\omega_n t}} \cos(\omega_D t')dt' \tag{III-15a}$$

$$B(t) = \frac{1}{m\omega_D} \int_0^t f_o(t') \frac{e^{\xi\omega_n t'}}{e^{\xi\omega_n t}} \sin(\omega_D t')dt' \tag{III-15b}$$

Then, we obtain the variance of $X(t)$ and compare it with the exact solution from (III-9a) to see if it agrees with the latter in an acceptable range. If so, we may conclude the simulation is good and what we want to do now is to solve (III-1) with $\mu \neq 0$, i.e. the nonlinear system.

Actually, there are many approximate methods to solve the nonlinear equation (III-1). The important thing is that we have to avoid large truncation errors which result in a divergent solution. This truncation error, sometimes called the discretization error, is dependent upon the selection of the interval size. We must choose the best approach to meet both economy and accuracy. We find the Runge-Kutta formula with truncation error of fifth order to be a very satisfactory method in this consideration. For steps smaller than some critical size [23], the higher error order gives less error.

Again, we compare the Runge-Kutta solution for the corresponding linear system with that from (III-15). When these studies are close, Runge-Kutta may be applied to solve (III-1). The variance of $X(t)$ will be found.

Risk Function and Reliability

The statistical property of X(t) has been obtained by the above analysis. Recalling that $S(t) = \bar{k}(X(t) + X^3(t))$, we obtain

$$\sigma_s^2 = \bar{k}^2\sigma_x^2 + 6\bar{k}^2\mu\sigma_x^4 + 15\,\bar{k}^2\mu^2\sigma_x^6 \qquad \text{(III-16)}$$

With this information, we can evaluate the reliability of the structure if we know the initial strength characteristics of the material.

In reliability theory, cessation of the performance of mechanical functions is called failure. These failures can be separated into two groups. First is the failure occurring as a result of stresses exceeding their limiting or critical values. The failure due to this reason is called first-passage failure. Second is the failure due to repeated loadings, i.e. fatigue. In this case, the loadings are not large enough to cause a failure of the first type but they do cause the successive incremental reduction of the limiting response. This means that repeated loadings hasten the reaching of first-passage. If the particular structure under consideration follows the power law for flaw propagation, (based upon the Griffith-Irwin equation as well as the Extreme Point Process), [19] we get the risk function, the probability of failure after a certain number of cycles, is as follows:

$$h_p(n) = \int_0^\infty \exp\left(\frac{-X^2}{2\sigma_s^2}\right) \frac{1}{\sqrt{2\pi}\,\sigma_n} \exp \frac{-(X-\bar{u}_n)^2}{2\sigma_n^2}\, dx \qquad \text{(III-17)}$$

where

$$\sigma_n^2 = \sigma_{R_o}^2 + \sigma_{Z_n}^2 \qquad \text{(III-17a)}$$

$$\bar{u}_n = \bar{R}_o - \bar{u}_{Z_n} \qquad \text{(III-17b)}$$

$\bar{R}_o$, $\sigma_{R_o}^2$ being the mean and variance of the initial resisting stress R_o

respectively, and $\bar{u}_{Z_n}$ and $\sigma^2_{Z_n}$ being the mean and variance of Z_n, $Z_n = \frac{K}{2} \sum_{j=1}^{n} S_j^3$ with S_j and the j-th peak of S(t) and independent of S_k for $j \neq k$ also, K is a propagation parameter.

Thus far, $\bar{R}_o$, $\sigma^2_{R_o}$, σ^2_S are known, but $\bar{u}_{Z_n}$ and $\sigma^2_{Z_n}$ are unknowns. To find $\bar{u}_{Z_n}$ and $\sigma^2_{Z_n}$, Crandall [24] first considered the stress process S(t) to consist of a sequence of half cycles each of duration π/ω_n and used Rice's definition of an envelope:

$$\bar{u}_{Z_n} = \frac{n}{2} K [\sqrt{2}\sigma_s]^3 \Gamma (1 + \frac{3}{2}) \qquad \text{(III-18a)}$$

$$\sigma^2_{Z_n} = \frac{n}{4} K [\sqrt{2}\sigma_s]^6 (1 - \Gamma^2 (1 + \frac{3}{2})) \qquad \text{(III-18b)}$$
$$+ \frac{1}{4} K^2[\sqrt{2}\sigma_s]^6 \Gamma^2 (1 + \frac{3}{2}) \times \{ \sum_{K=1}^{M-1} (M-k)[H(-\frac{3}{2},-\frac{3}{2};1,r^{*2}(\tau))-1]\}$$

Here, H is the hypergeometric function and

$$r^*(\tau) = \frac{2}{\sigma_s^2} [(\int_0^\infty \phi(\omega)|H(\omega)|^2 \cos(\omega-\omega_n)\tau d\omega)^2 \qquad \text{(III-19)}$$
$$+ (\int_0^\infty \phi(\omega)|H(\omega)|^2 \sin(\omega-\omega_n)\tau d\omega)^2]^{1/2}$$

$\phi(\omega)|H(\omega)|^2$ is the spectral density of the process X(t).

It is clear that the further evaluation of $\sigma^2_{Z_n}$ requires the value of $r^*(\tau)$ to specify the parameter of the hypergeometric function. This is a laborious task. One way to overcome this difficulty is to consider the case of small damping and to assume the argument of the hypergeometric function is oscillating with period π/ω_n. This is limited to white-noise type excitations, but it can be treated as an approximate value for another type of excitation, especially when the damping is small, so the complex-frequency response $H(\omega)$ is very sharply peaked at about ω_n. Thus (III-18b) is approximated as:

$$\sigma_{Z_n} = 0.092 \frac{n}{\xi} K^2[\sqrt{2}\ \sigma_s]^6 \Gamma^2 (2.5) \qquad \text{(III-20)}$$

Now we are able to calculate (III-17). However, numerical integration needs thousands of operations with a high-speed digital computer. We derive the following formula from (III-17) to simplify the evaluation:

$$h_p(n) = \frac{1}{2\sqrt{2}\,\sigma_n W} \exp\left[-\frac{\bar{u}_n^2}{2\sigma_n^2}\left(1 - \frac{1}{2\sigma_n^2 W^2}\right)\right]\left(\sqrt{2} + \operatorname{erf}\left(\frac{\bar{u}_n}{2\sigma_n^2 W}\right)\right) \qquad \text{(III-21)}$$

where $W^2 = \frac{1}{2\sigma_s^2} + \frac{1}{2\sigma_n^2}$, and erf is the error function which can be obtained by the asymptotic series

$$\operatorname{erf}(x) = 1 - \frac{1}{\sqrt{\pi}} e^{-x^2}\left(\frac{1}{x} - \frac{1}{2x^3} + \frac{1.3}{2^2 x^5} - \ldots\right) \qquad \text{(III-21a)}$$

Thus the reliability of a structure which will survive N stress cycles is

$$L(N) = \prod_{n=0}^{N-1} [1 - h_p(n)]$$

$$\doteq \exp\left[-\sum_{n=0}^{N-1} h_p(n)\right] \qquad \text{for } h_p(n) \ll 1 \qquad \text{(III-22)}$$

A Numerical Example -- Wind Pressure on a Structure

As an example, let m = 1 kip sec^2/in and ω_n = 1.732 rad/sec for the system described by (1) and assume the system starts from rest, i.e. with initial conditions $X(t) = \dot{X}(t) = 0$. The system is excited by a strong gust whose spectrum is described by Davenport's [25] empirical formula:

$$S_V(f)df = 4CV^2 \frac{x}{(1 + x^2)^{4/3}}\, dx \qquad \text{(III-23)}$$

where

$x = 4000 \frac{f}{V}$ (cycle/foot)

V = a standard velocity of wind at 33 feet height

C = a resistance coefficient of the ground surface. In terrain

uniformly covered with obstacles 30 - 50 feet in height, i.e. residential suburbs, small towns, etc. C = 0.015.

So, the spectral density of the fluctuating part of the wind pressure on the structure may be assumed as

$$\phi(f) = \frac{(\rho_a V C_D)^2}{f} 4CV^2 \frac{x^2}{(1 + x^2)^{4/3}} \qquad \text{(III-24)}$$

C_D = pressure coefficient = 0.5 [26]

Figure 6 shows (III-24).

In the following process of calculation, we must always recall that $\omega = 2\pi f$, because (III-24) is expressed in cycles, but in the previous analyses the formula are in radians.

From (III-13), (III-13a), (III-14) and (III-14a), we get

$$\omega_i = 2\pi f_i = 2\pi \frac{V}{4000} \left[\left(\frac{1}{1-r_i}\right)^3 - 1\right]^{1/2} \qquad i = 1,\ldots N \qquad \text{(III-25)}$$

With the aid of (III-12), (III-13a), and (III-25), a typical simulated excitation with wind velocity V = 120 ft/sec and N = 250 is shown in Fig. 7.

1. Monte Carlo Simulation

Fig. 8 shows the comparison between different approaches for the corresponding linear system. The triangles indicate the exact solution from (III-9a) and crosses denote solutions from the Duhamel Equation (III-15) based upon the simulated excitation (III-12). If the simulation (III-12) is good, these values should be very close. Actually the technique of simulation (III-12) is dependent on the selection of size, the number of cosine terms, and the time duration for computing the variance. These factors will be discussed later. From Fig. 8, we may conclude that the simulation is fairly acceptable. The results of Fig. 8 at the same time

indicate the accuracy of the Runge-Kutta Method for solving (III-1) with the excitation (III-12) on a step-by-step timewise basis. Fig. 9 shows a typical simulated result using these two approximate methods. The fact the numerical results are too close to plot as two distinct curves reflects the feasibility of the present analysis. The computing time for this approach was 50.67 seconds.

2. Perturbation Approach

Figs. 10 to 15 show a series of nonlinear responses each with a different value of μ. For this system: (A) If μ is smaller than 0.2 the perturbation method is seen to be reasonable agreement with the Monte Carlo simulation for lower values of excitations. On the other hand, some simulated solutions (Figs. 10, 11, and 12) seem to be unreliable because their values are higher than those of the corresponding linear system shown in Fig. 8 and reproduced in Figs. 10, 11, and 12. This is due to the fact we used the larger time interval (0.4 sec.) for higher excitations which caused a little divergence when we applied the Runge-Kutta formula. This deviation can be reduced when the nonlinearity increases. (See Figs. 13 and 14) (B) If μ is larger than 0.2, application of the perturbation method will cause an unacceptable error, as shown in Fig. 14. However, in this case, the simulated approach does have a great advantage. All data are plotted in Fig. 15.

Fig. 16 describes the corresponding linear system with various damping ratios. It is quite clear that the higher the damping ratio the closer these two methods agree. This hints that the perturbation method will do well when $\mu = 0.3$ (or larger) and simulated solutions will be good at higher excitations even with a larger interval size such as 0.4 sec. These are showed in Figs. 17 and 18. The computing time for the perturbation approach was 2.67 seconds.

Here, considering the case of $\xi = 0.02$ and $\mu = 0.05$ and V = 100 ft/sec, ($\sigma_f^2 = 0.5136$ in^2) we get $\sigma_x = 0.284$ in from Fig. 11. Applying (III-16), we obtain:

$$\sigma_s^2 = 0.744 \text{ in}^2 \qquad \sigma_s = 0.862 \text{ in} \qquad \text{(III-26)}$$

If the mean of the initial resistance, $\bar{R}_0$ is 3.45 kips and the propagation parameter K for this system is 2.435×10^{-5}, with the aid of (III-18a), (III-20), (III-21) and (III-26), we obtain the estimates of the risk function $h_p(n)$ which is the curve A in Fig. 19. The reliability is carried out by (III-22) and is shown by curve A in Fig. 20. Furthermore, we consider the statistical variation of the initial strength R_0. Curves B and C in Figs. 19 and 20 represent the results for variations of five and ten percent respectively. Similarly, in each of these two figures curve D, E and F are obtained for $\bar{R}_0 = 3.85$ kips and variations 0, five and ten percent respectively.

Conclusions

Although the approaches presented are developed for (III-1), they can be extended to other nonlinear systems by the same proceudres. From the view point of computing for the specific example used, the perturbation method is more efficient than the Monte Carlo method. The perturbation method takes only about one-twentieth the computing time that is needed for the Monte Carlo simulation technique. In general, when the perturbation parameter is small, the method works well. However, if the damping ratio increases or the excitation decreases, the method still proves to be adequate even if the perturbation parameter is large. This can be explained by the fact that the system has only slight nonlinearity.

Notation used in Chapter III

$X(t)$, X, X_i $i=1,2\ldots$	Displacement Response Function
$E[\ ]$	Ensemble average or expectation
$S(t)$	Stress response function
S_j	The j-th peak of $S(t)$
ω_n	Natural frequency of corresponding linear system
ω_D	Damped vibration frequency
T	Fundamental Period
m	Mass of structure
ξ	Damping ratio
μ	Perturbation of nonlinear parameter
$\bar{k}$	Stiffness of structure
R_o	Initial strength of structure
$\bar{R}_o$	Mean of R_o
$\sigma_{X_o}, \sigma_X, \sigma_S, \sigma_{R_o}$	Standard deviation of X_o, X, $S(t)$, and R_o respectively
$f(t)$	Generalized force, excitation
$f_o(t)$	Simulation of $f(t)$
$\sigma(\omega)$	Spectral density function of $f(t)$
σ_f^2	Variance of $f(t)$
R_f	Autocorrelation function for $f(t)$
$h(\theta)$	Impulse-response function
$H(\omega)$	Complex-frequency response
$g(\omega)$	Probability density function for ω
$F_g(\omega)$	Cumulative distribution function of $g(\omega)$
$F_g^{-1}(\omega)$	Inverse function of $F_g(\omega)$

r, r_i	Generating random numbers, i = 1,2,...N
K	Propagation parameter
$h_\rho(n)$	Risk function, probability of structure's failure after n stress cycles
H	Hypergeometric function
V	Wind velocity
L(N)	Reliability of structure
Z_n	$K/2 \sum_{j=1}^{n} S_j^3$
$\bar{u}_{Z_n}$	Mean of Z_n
$\sigma^2_{Z_n}$	Variance of Z_n
C	Resistance coefficient of ground surface
C_D	Pressure coefficient
$S_v(f)$	Spectrum of wind velocity
ρ_a	Density of air, 0.0024 slug/ft^3

CHAPTER IV

RESPONSE OF A NONLINEAR SYSTEM TO NONSTATIONARY RANDOM EXCITATION

Introduction

The transient mean-square response of a linear single-degree-of-freedom mechanical system to certain types of nonstationary random excitation has been studied by many authors [27,28,29,30]. The nonstationary input was taken in the form of a product of a well-defined envelope function, A(t) and a stationary Gaussian noise with zero mean, n(t).

Caughey and Stumpf [27] have examined the case in which the envelope function A(t) is a unit step function and n(t) is assumed to be either white noise or broad-band noise whose power spectral density has no sharp peaks. Results of their analysis were applied to the determination of the structural response to earthquake ground motion. Bolotin [28] has determined the mean-square response of a structure represented by a second order differential equation to earthquake excitation. In his analysis, he considered the ground acceleration to be characterized by the product of an exponentially decaying harmonic correlation function and an envelope function, $A(t) = Ae^{-ct}$.

In a recent paper [29], Barnoshi and Maurer have formulated the time varying mean-square response of a linear single-degree-of-freedom system in terms of the system frequancy response function and the generalized spectral density function of the input excitation. They considered the envelope function to be either the unit step function or a rectangular step function. Bucciarelli and Kuo [30] have recently obtained an approximate expression for the mean-square response to excitation characterized by a general envelope function subject only to the restriction that the envelope function is slowly varying. Their work also gave an

estimated maximum value of the mean-square response.

In all the above studies, the systems treated were linear. The present study presents an approximate solution to the problem of transient mean-square response of a simple nonlinear system to a non-stationary random excitation. Only systems with geometric nonlinearities (rather than materials nonlinearities) are considered and the nonlinear differential equation is linearized by an equivalent linearization technique. The results are directly applicable to determination of response of an elastic flat rectangular or circular plate subject to random lateral loading when the plate is approximated as a single-degree-of-freedom system characterized by its central deflection. Obviously the results also apply to other one-degree-of-freedom mechanical systems excited by nonstationary random forces.

Analysis

Consider a lightly damped single-degree-of-freedom mechanical system subjected to a random excitation and governed by the equation

$$\ddot{y}(t) + 2\zeta\omega_n\dot{y}(t) + \omega_n^2(y) + g(y)) = f(t) \qquad \text{(IV-1)}$$

where

ζ = fraction of critical damping

ω_n = natural frequency of the corresponding linear system

$$g(y) = \sum_{k=1}^{N} \mu_k y2k+1 \qquad \mu_k \geq 0 \qquad \text{(IV-2)}$$

The nonstationary random excitation f(t) is expressed by

$$f(t) = A(t)n(t) \qquad \text{(IV-3)}$$

where A(t) is a well-defined envelope function and n(t) is a Gaussian stationary random process with zero mean and autocorrelation function $R_n(\tau)$.

We are to determine the mean-square response $E[y^2(t)]$ to an input $f(t)$ when the envelope function is a unit step function:

$$A(t) = u(t) \tag{IV-4}$$

and $n(t)$ has the autocorrelation functions

$$R_n(\tau) = 2\pi K_o \delta(\tau) \tag{IV-5}$$

Although various methods can be applied to determine the response of nonlinear systems, the equivalent linearization technique will be used here. This technique was developed by Krylov and Bogoliuvov for the treatment of nonlinear systems under deterministic excitations, and then Booton [31] and Caughey [32] applied this technique to problems of random vibrations.

We assume that an approximate solution of (IV-1) can be obtained from the linearized equation

$$\ddot{y} + 2\beta_e \dot{y} + \omega_e^2 = f(t) \tag{IV-6}$$

where β_e is the equivalent linear damping coefficient and ω_e^2 is the equivalent linear stiffness. The error "e" due to linearization is given by the difference between (IV-1) and (IV-6), i.e.,

$$e = 2(\zeta\omega_n - \beta_e)\dot{y} + (\omega_n^2 - \omega_e^2)y + g(y)\omega_n^2 \tag{IV-7}$$

The variables β_e and ω_e^2 are chosen so as to minimize the mean-square error $E[e^2]$. The resulting values involve $E[y^2]$, $[\dot{y}^2]$ and $E[y\dot{y}]$, hence it is necessary to know the probability density function $p(y,\dot{y})$. In general, however, $p(y,\dot{y})$ is not known. If the input is Gaussian and the nonlinearities of the system are small, then the response of the linearized equation (III-6) is also Gaussian. Therefore, the assumption is made that the probability density function $p(y,\dot{y})$ is Gaussian with covariances to be determined. Before constructing the probability density function, however, it is necessary to find ensemble averages of y and $\dot{y}$

and these are readily found by Duhamel's integral to be

$$E[y] = \int_0^t h(t-\tau)E[f(\tau)]d\tau \qquad \text{(IV-8)}$$

and if we assume that $E[f(t)] = 0$, then

$$E[y] = 0 \qquad \text{(IV-9)}$$

Similarly, the ensemble average of y is obtained as

$$E[\dot{y}] = \int_0^t \frac{\partial}{\partial t} h(t-\tau)E[f(\tau)]d\tau \qquad \text{(IV-10)}$$

$$= 0$$

Thus, the assumed Gaussian probability density function $p(y,\dot{y})$ takes the form

$$p(y,\dot{y}) = \frac{1}{2\pi(\det(K))^{1/2}} \exp(-ay^2 + 2by\dot{y} - c\dot{y}^2) \qquad \text{(IV-11)}$$

where

$$\begin{aligned} a &= E[\dot{y}^2]/(2\det(K)) \\ b &= E[y\dot{y}]/(2\det(K)) \\ c &= E[y^2]/(2\det(K)) \\ \det(K) &= E[y^2]E[\dot{y}^2] - (E[y\dot{y}])^2 \end{aligned} \qquad \text{(IV-12)}$$

This leads to

$$2\beta_e = 2\zeta\omega_n \qquad \text{(IV-13)}$$

$$\omega_e^2 = \omega_n^2 \left\{1 + \sum_{k=1}^{N} \mu_k \frac{(2k+1)!}{2^k k!} (E[y^2])^k \right. \qquad \text{(IV-14)}$$

It is interesting to observe that the above equivalent linear damping $2\beta_e$ and stiffness ω_e^2 are identical to those found for a stationary process in which case $E[y\dot{y}]$ is equal to zero.

If the nonlinearity is involved only in the velocity term such as $g(\dot{y})$ it is possible to demonstrate thatthe equivalent linear damping and stiffness for a nonstationary process are identical to those for a stationary process.

In all cases, the mean-square response $E[y^2]$ at any time t is obtained from the expected value of $(y(t))^2$ over the ensemble response. Use of Duhamel's integral leads to

$$E[y^2] = \frac{1}{\omega_d^2}\int_0^t\int_0^t \exp\{-\zeta\omega_n(2t-\tau-\tau')\}\sin\omega_d(t-\tau')\sin\omega_d(t-\tau)A(\tau)A(\tau') \cdot$$

$$\cdot R_n(\tau-\tau')d\tau d\tau' \qquad \text{(IV-15)}$$

where

$$\omega_d^2 = \omega_n^2\{1 + \sum_{k=1}^{N} \mu_k \frac{(2k+1)!}{2^k k!}(E[y^2])^k - \zeta^2\} \qquad \text{(IV-16)}$$

If the input is white noise, then (IV-15) becomes

$$E[y^2] = \frac{\pi K_o}{\omega_d^2}\int_0^t \exp\{-2\zeta\omega_n(t-\tau)\}\sin^2\omega_d(t-\tau)d\tau$$

$$= \frac{\pi K_o}{4\zeta\omega_n(\zeta^2\omega_n^2+\omega_d^2)}[1 - e^{-2\zeta\omega_n t}(1 + \frac{2\zeta^2\omega_n^2}{\omega_d^2}\sin^2\omega_d t + \frac{\zeta\omega_n}{\omega_d}\sin^2\omega_d t)] \qquad \text{(IV-18)}$$

Employing (IV-16), (IV-18) becomes a nonlinear algebraic equation for $E[y^2]$ since ω_d^2 is a function of $E[y^2]$ in (IV-16). This type of equation generally has more than one solution. However, from physical considerations the desired solution will be that one close to the solution of the corresponding linear system because only a weakly nonlinear system is being considered. It is convenient to solve this system through use of Newton's method of tangents together with iteration. As an example, let us consider the case

$$g(y) = \mu y^3 \qquad \text{(IV-19)}$$

For various values of μ and damping coefficient ζ, $E[y^2]$ is computed and the normalized plots such as shown in Figure 21 result. The normalization factor is determined by the stationary mean-square response of the linear system

$$E[y_o^2] = \pi K_o/4\zeta\omega_n^3 \tag{IV-20}$$

The parameter μ is chosen in such a manner that given μ the stationary mean-square response reaches 40 percent, 60 percent and 80 percent of $E[y_o^2]_s$.

If the damping is small, (IV-18) can be approximated by

$$E[y^2] \approx E[y_o^2]_s \frac{(1 - e^{-2\zeta\omega_n t})}{1 + 3\mu E[y^2]} \tag{IV-21}$$

from which the following approximate solution is obtained:

$$E[y^2] \approx \frac{1}{6\mu}\{[1 + 12\mu E[y_o^2]_s(1 - e^{-2\zeta\omega_n t})]^{1/2} - 1\} \tag{IV-22}$$

From the above results it is easy to demonstrate that the transient mean-square response for both linear and nonlinear systems does not exceed the stationary mean-square response to white noise.

If instead of (IV-5) the function n(t) has the autocorrelation

$$R_n(\tau) = K_o \exp(-\alpha|\tau|)\cos\beta\tau \tag{IV-23}$$

(termed correlated noise) then (IV-15) becomes

$$E[y^2] = \frac{K_o e^{-2\zeta\omega_n t}}{\omega_d^2} \int_0^t\int_0^t \exp[\zeta\omega_n(\tau+\tau') - \alpha|\tau-\tau'|]A(\tau)A(\tau')\sin\omega_d(t-\tau)$$

$$\sin\omega_d(t-\tau')\cos\beta(\tau-\tau')d\tau d\tau' \tag{IV-24}$$

Use of (IV-4) in (IV-24) leads to the desired expression for $E[y^2]$. In the interest of brevity this lengthy expression is not given. However, inspection of it reveals that the mean-square response depends upon interrelationships between damping ζ, the corresponding linear system natural frequency ω_n, the decay constant and the frequency β of the correlation function.

For a white noise input, only the value of damping of the system influences the time required to attain stationarity. However, for the

correlated noise input, the time required for the response to reach a stationary value is influenced not only by the system damping coefficient ζ but also by the decay constant α of the input noise. Inspection of results indicates that as α decreases, i.e. the power spectral density has a sharp peak at some frequency, then the transient response tends to exceed the stationary value. Another interesting result is that the nonlinear response becomes greater than the corresponding linear response under certain conditions even if the system has hardening spring-type nonlinearity. An example of this is shown in Figure 22.

Conclusions

The time varying mean-square response of a nonlinear single-degree-of-freedom mechanical system to nonstationary random excitation characterized by the product of an envelope function and a stationary Gaussian random process has been considered. A unit step envelope function was considered in conjunction with both correlated and white noise with zero mean. The nonlinear governing equation was linearized by the method of equivalent linearization.

For the nonstationary process it has been shown that the equivalent linear damping coefficient and the equivalent linear stiffness for the system with nonlinearities involved only in displacements or only in velocities are the same as those for the stationary process.

The mean-square response depends upon the coefficients of the system equation, the shape of the envelope function, and the parameters of the autocorrelation of the process $n(t)$. It was proved that for white noise modulated by a unit step function, the transient mean-square response never exceeds the stationary response. However, the mean-square response to

correlated noise modulated by a unit step function may exceed its stationary value, especially when the power spectral density of the process n(t) has a sharp peak, and its maximum value becomes several times the stationary value.

It has also been shown that the mean-square response of the system with cubic hardening spring-type nonlinearity may be greater than the corresponding linear system response under certain conditions.

The results presented are directly applicable to determination of response of a single-degree-of-freedom mechanical system to nonstationary random excitation. In the case of a flat rectangular plate subject to random lateral loading the response at the center of the plate is frequently the one of greatest interest and in this case the vibrating plate may be represented as a one-degree-of-freedom system.

CHAPTER V

ADMINISTRATIVE ASPECTS OF THE GRANT

Publication

1. Tai, I.H. and William A. Nash, "Vibrations of Thin Plates - A New Approach," AFOSR-TR-74-0789, December, 1973. University of Massachusetts, Amherst, Massachusetts.

2. O'Callaghan, M.J.A., William A. Nash and P.M. Quinlan, "Vibrations of Thin Elastic Shells - A New Approach," AFOSR-TR-76-0731, August, 1975. University of Massachusetts, Amherst, Massachusetts.

3. Kanematsu, H., and William A. Nash, "Mean-Square Response of a Non-Linear System to Nonstationary Random Excitation," AFOSR Report, August, 1976. University of Massachusetts, Amherst, Massachusetts.

4. Tai, I.H. and William A. Nash, "Vibrations of Thin Elastic Plates - A New Approach," Proceedings of the Fifth Canadian Congress of Applied Mechanics, 1975, pp. 281-282.

5. O'Callaghan, M.J.A., William A. Nash and P.M. Quinlan, "Vibrations of Thin Elastic Shells - A New Approach," International Association of Space Structures, Proceedings of the World Congress on Space Enclosures, Montreal, 1976, pp. 377-382, Vol. 1.

6. Nash, W.A. and H. Kanematsu, "Dynamic Response of Elastic Plates Subject to Nonstationary Random Excitation," Transactions of the Third International Conference on Structural Mechanics in Reactor Technology, Vol. 2, Part F, London, 1975, pp. F8/7, 1-7.

Students Associated with the Grant

I.H. Tai, who received the Ph.D. in 1973.

H. Kanematsu, who received the Ph.D. in 1972.

Y.C. Tan, who received the M.S. in 1976.

M.J.A. O'Callaghan, post-doctoral research associate.

REFERENCES

1. Leissa, A.W., VIBRATION OF PLATES, NASA SP-160, 1969.

2. Quinlan, P.M., The λ Method for Skew Plates, Proc. Fourth U.S. Nat. Congr. of Appl. Mech., 1962.

3. Quinlan, P.M., The Torsion of an Irregular Polygon., Proc. Roy. Soc., Vol. 282A, 1964.

4. Quinlan, P.M., The λ Method for Rectangular Plates, Proc. Roy. Soc., Vol. 288A, 1964.

5. Quinlan, P.M., Plates with Polygonal or Curved Boundaries with Holes, OAR Research Report, 1967.

6. Quinlan, P.M., Polygonal and Swept-back Plates with Cut-outs and Column Supports, OAR Research Applications Conference, March 1968.

7. Tai, I.H., and William A. Nash, "Vibrations of Thin-Plates - A New Approach," AFOSR-TR-74-0789, December, 1973. University of Massachusetts, Amherst, Massachusetts.

8. Tomotika, S., The Transfer Vibration of a Square Plate Clamped at Four Edges, Phil. Mag., Ser. 7, Vol. 21, No. 142, April 1936, pp. 745-760.

9. Young, D., Vibration of Rectangular Plates by the Ritz Method, J. Appl. Mech., Vol. 17, No. 4, December, 1950, pp. 448-453.

10. Iguchi, S., Die Eigenwert Probleme Fur Die Elastische Rechteckige Platte, Mem. Fac. Eng., Hokkaido Univ., 1938, pp. 305-372.

11. Kraus, H., Thin Elastic Shells, John Wiley and Sons, New York, 1967.

12. O'Callaghan, M.J.A., "The Edge-Function Method for Linear Boundary Problems with Discontinuous Boundary Conditions," Ph.D. Thesis, University College, Cork, Ireland, 1972.

13. O'Callaghan, M.J.A., William A. Nash and P.M. Quinlan, "Vibrations of Thin Elastic Shells - A New Approach," AFOSR-TR-76-0731, August, 1975. University of Massachusetts, Amherst, Massachusetts.

14. Vlazov, V.A., General Theory of Shells and its Applications in Engineering (in Russian). Translated into English as NASA-TT-F99, 1964.

15. Malkina, R.L., "Vibrations of Spherical Shells," (in Russian). Izv. Vys. Uch. Zav. Avia. Tekh. No. 1, 1964, pp. 64-74.

16. Crandall, S.H., Perturbation Techniques for Random Vibration of Nonlinear System, J. Acoust. Soc. of America, 1963.

17. Lin, Y.K., Probabilistic Theory of Structural Dynamics, McGraw Hill, 1967.

18. Shinozuka, M., Simulation of Multivariate and Multidimensional Random Processes, J. Acoust. Soc. of America, 1970.

19. Yang, J.N. and Heer, E., Reliability of Randomly Excited Structures, J. AIAA, 1971.

20. Crandall, S.H. and Mark, W.D., Random Vibration in Mechanical Systems, Academic, N.Y., 1963.

21. Naylor, T.H. and others, Computer Simulation Techniques, John Wiley & Son, 1966.

22. Clough, R.W. and Penizien, J., Dynamics of Structures, McGraw-Hill, 1975.

23. Crandall, S.H., Engineering Analysis - A Survey of Numerical Procedures, McGraw-Hill, 1956.

24. Crandall, S.H., Mark, W.D. and Khabbaz, G.R., The Variance in Palmgren-Miner Damage Due to Random Vibration, 4th U.S. National Congress of Applied Mech., Vol. 1, 1962.

25. Davenport, A.G., The Application of Statistical Concepts to the Wind Loading of Structures, Proc. Inst. Civil Eng., Vol. 19, 1961.

26. Wen, Y.K. and Shinozuka, M., Monte Carlo Solution of Structural Response to Wind Load, 3rd International Conference on Wind Effects on Buildings and Structures, Tokyo, 1971.

27. Caughey, T.K. and Stumpf, H.J., "Transient Response of a Dynamic System Under Random Excitation," Journal of Applied Mechanics, 28, 4, 1961.

28. Bolotin, V.V., "Statistical Methods in Structural Mechanics," Translated by S. Aroni, Holden-Day, Inc., San Francisco, 1969.

29. Barnoski, R.L. and Maurer, J.R., "Mean-Square Response of Simple Mechanical Systems to Nonstationary Random Excitation," Journal of Applied Mechanics, 36, 2, 1969.

30. Bucciarelli, L.L. and Kuo, C., "Mean Square Response of a Second-Order System to Nonstationary Random Excitation," Journal of Applied Mechanics, 37, 3, 1970.

31. Booton, R.C., "The Analysis of Nonlinear Control Systems with Random Inputs, Proceedings of the Symposium on Nonlinear Circuit Analysis, Vol. II, 1953.

32. Caughey, T.K., "Equivalent Linearization Techniques," Journal of the Acoustical Society of America, 35, 11, 1963.

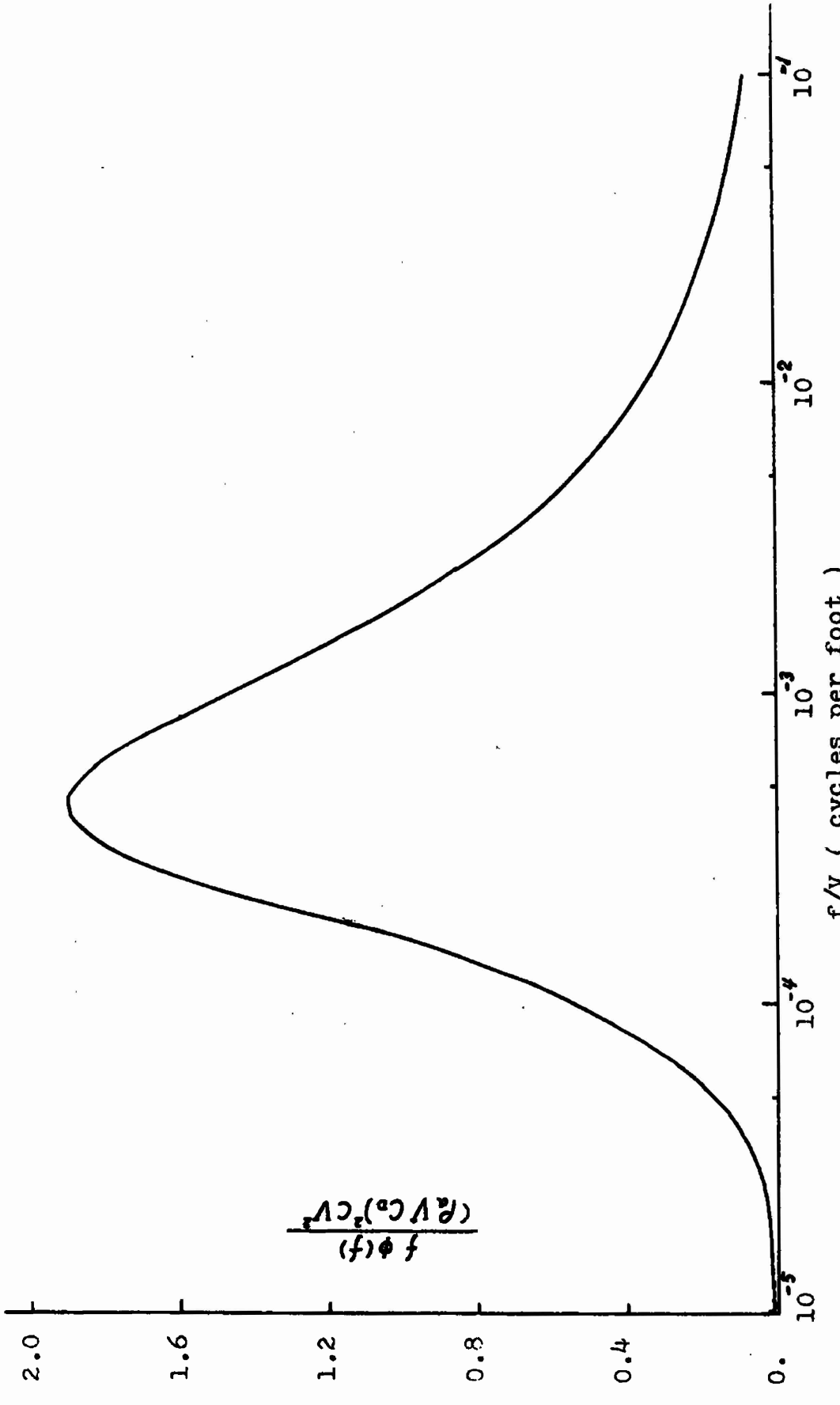

Fig. 6. Spectral density function of wind pressure

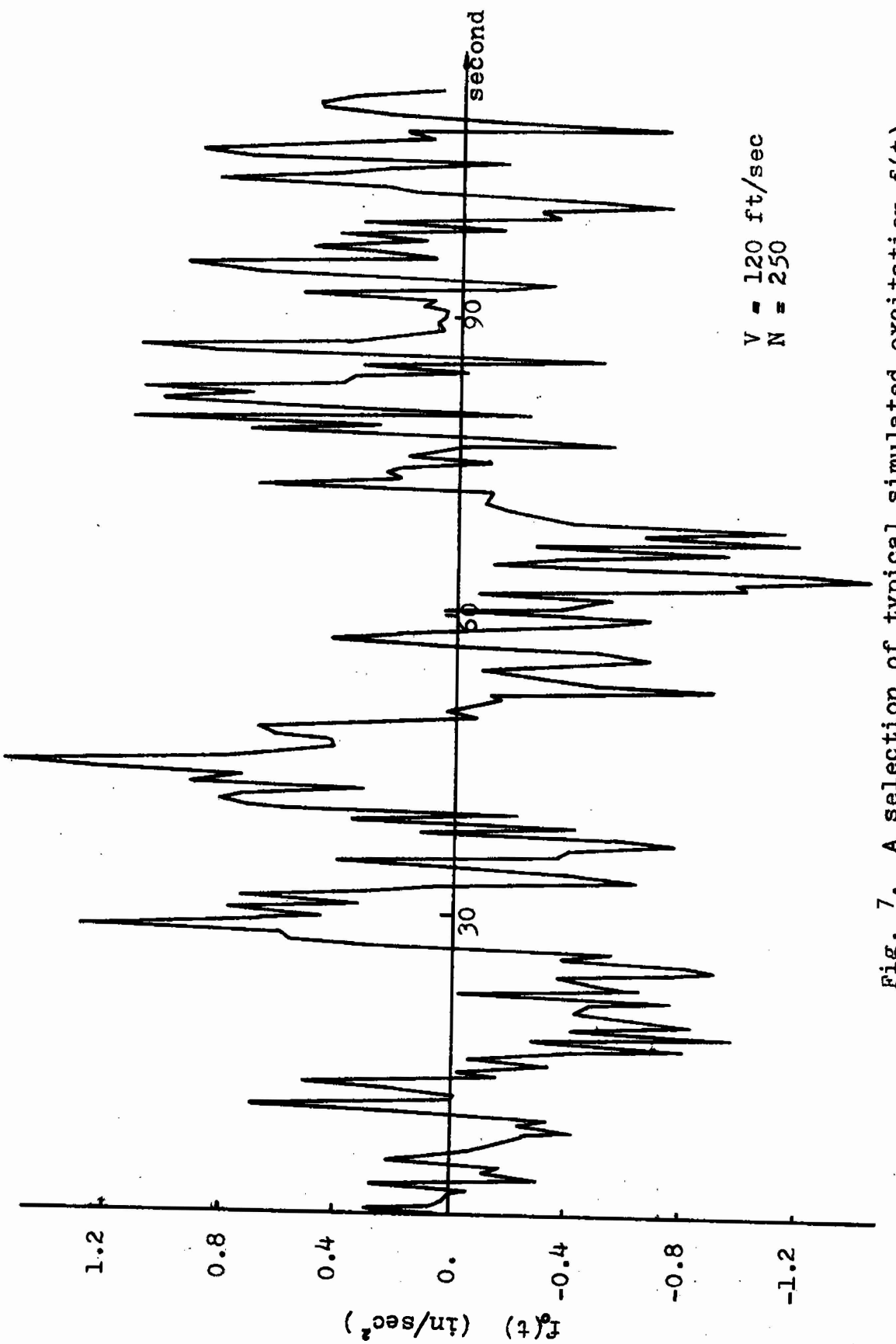

Fig. 7. A selection of typical simulated excitation $f_\delta(t)$

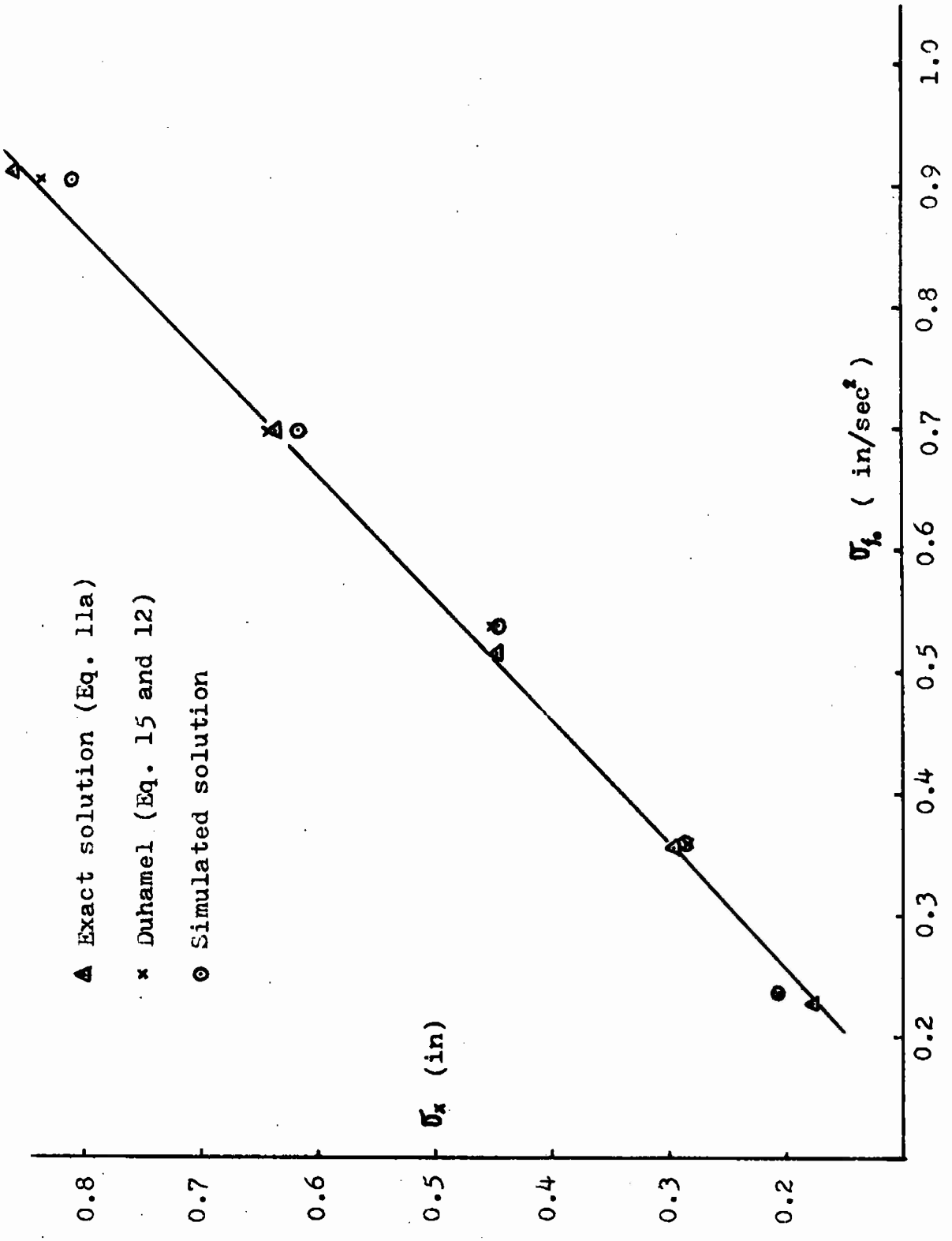

Fig. 8. RMS response of system to excitation with $\zeta = 0.02$ and $u = 0$

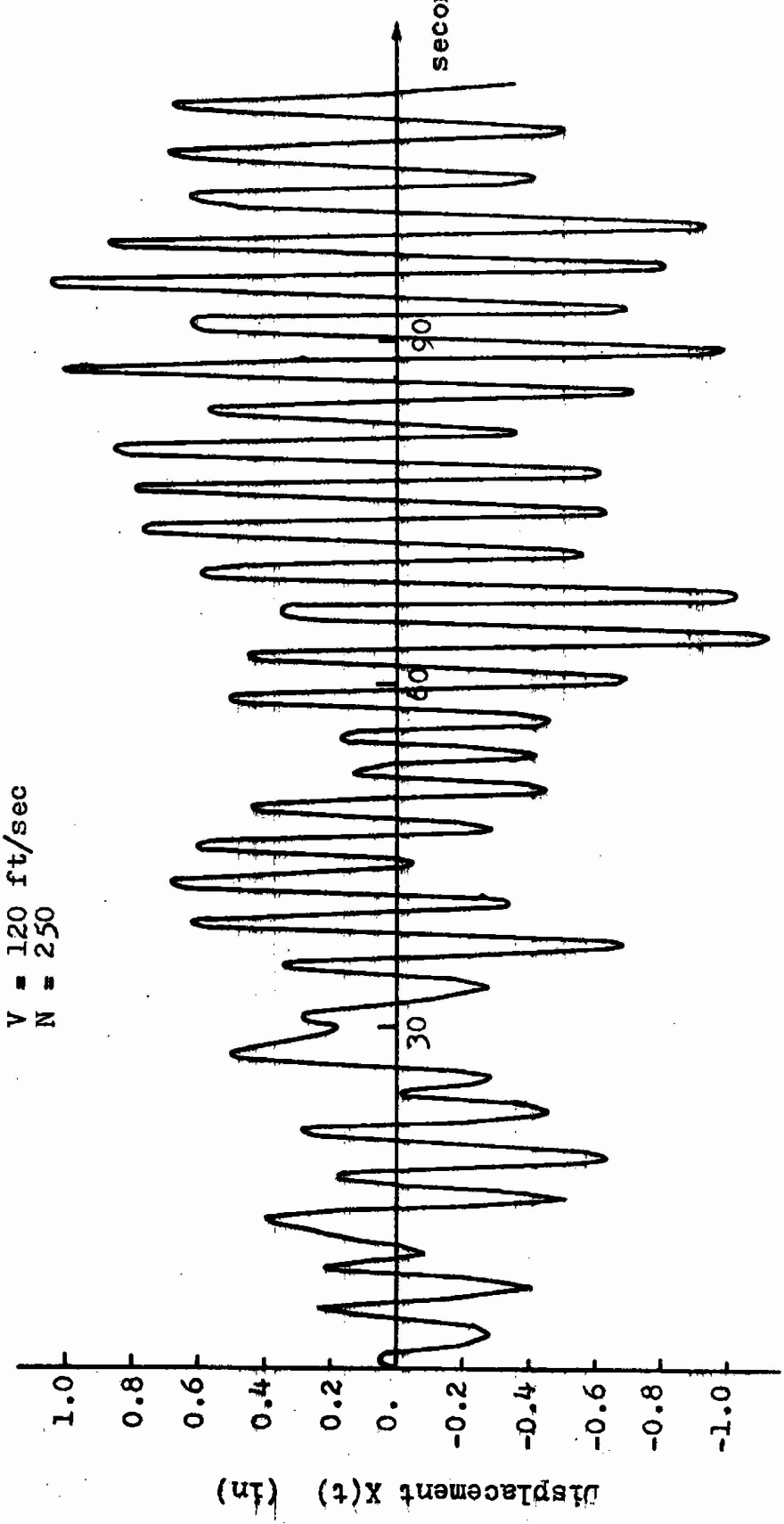

Fig. 9. A selection of typical simulated response

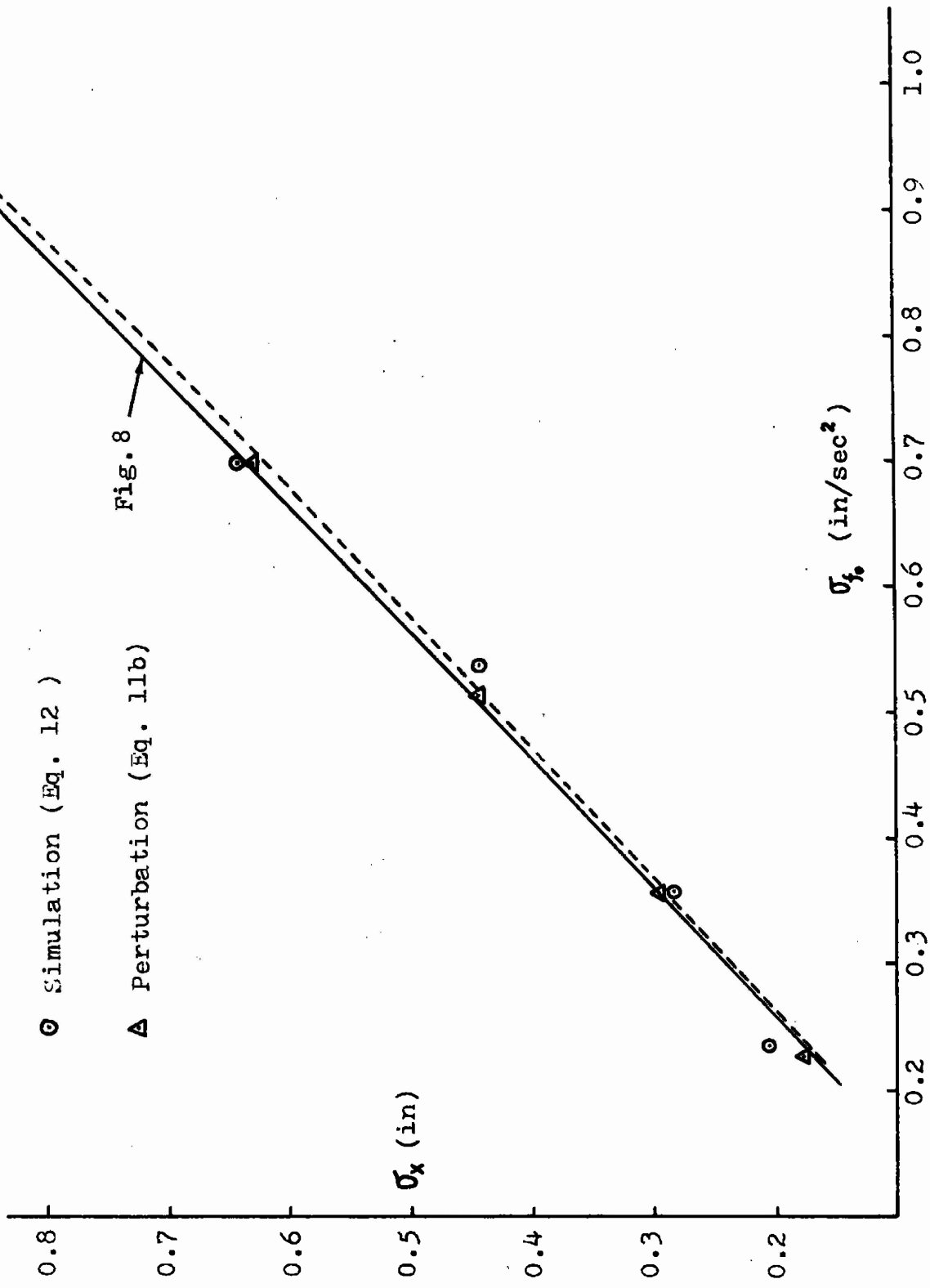

Fig. 10. RMS response of system to excitation with $\zeta = 0.02$ and $u = 0.01$

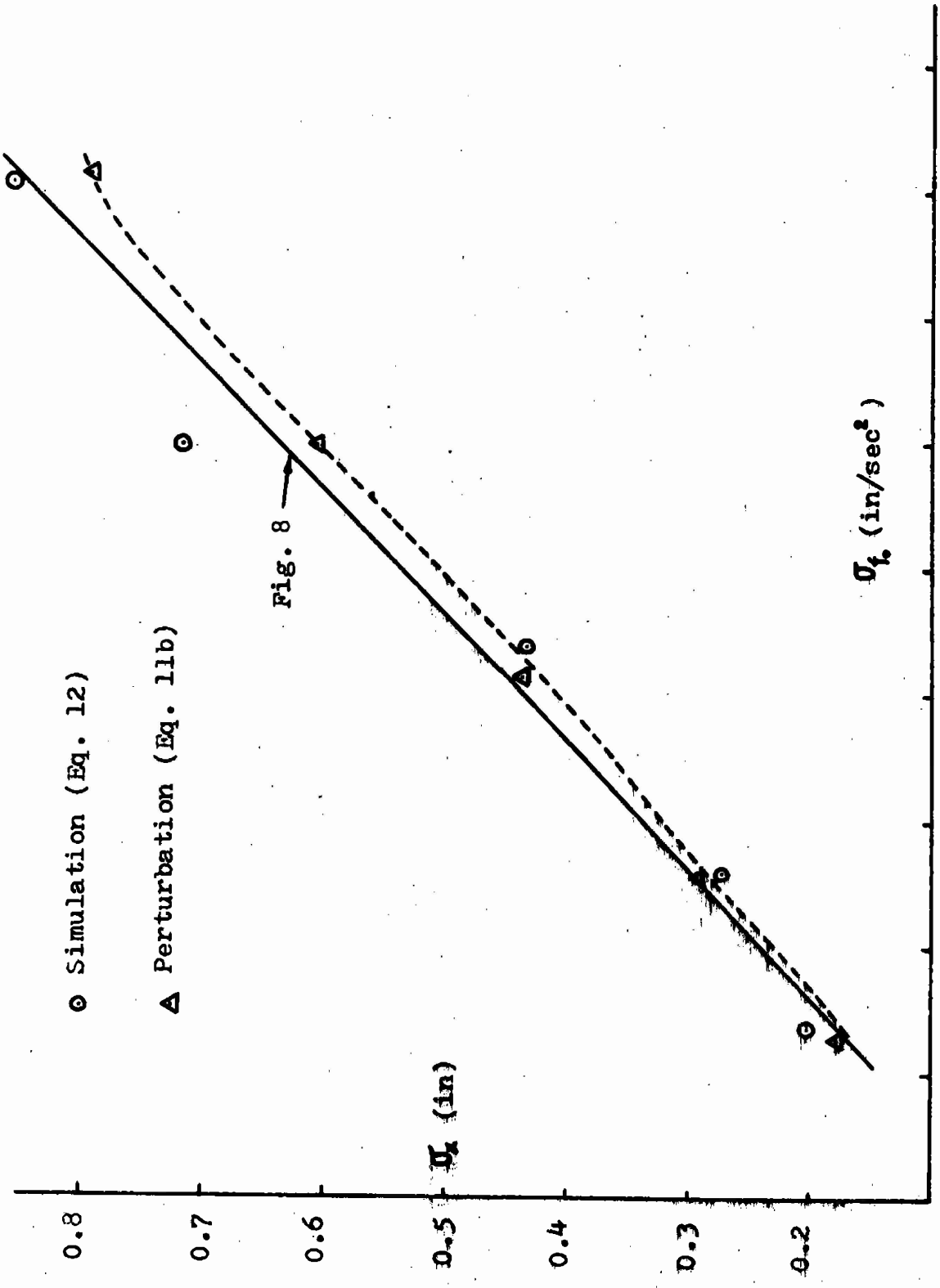

Fig. 11. RMS response of system to excitation with $\zeta = 0.02$ and $u = 0.05$

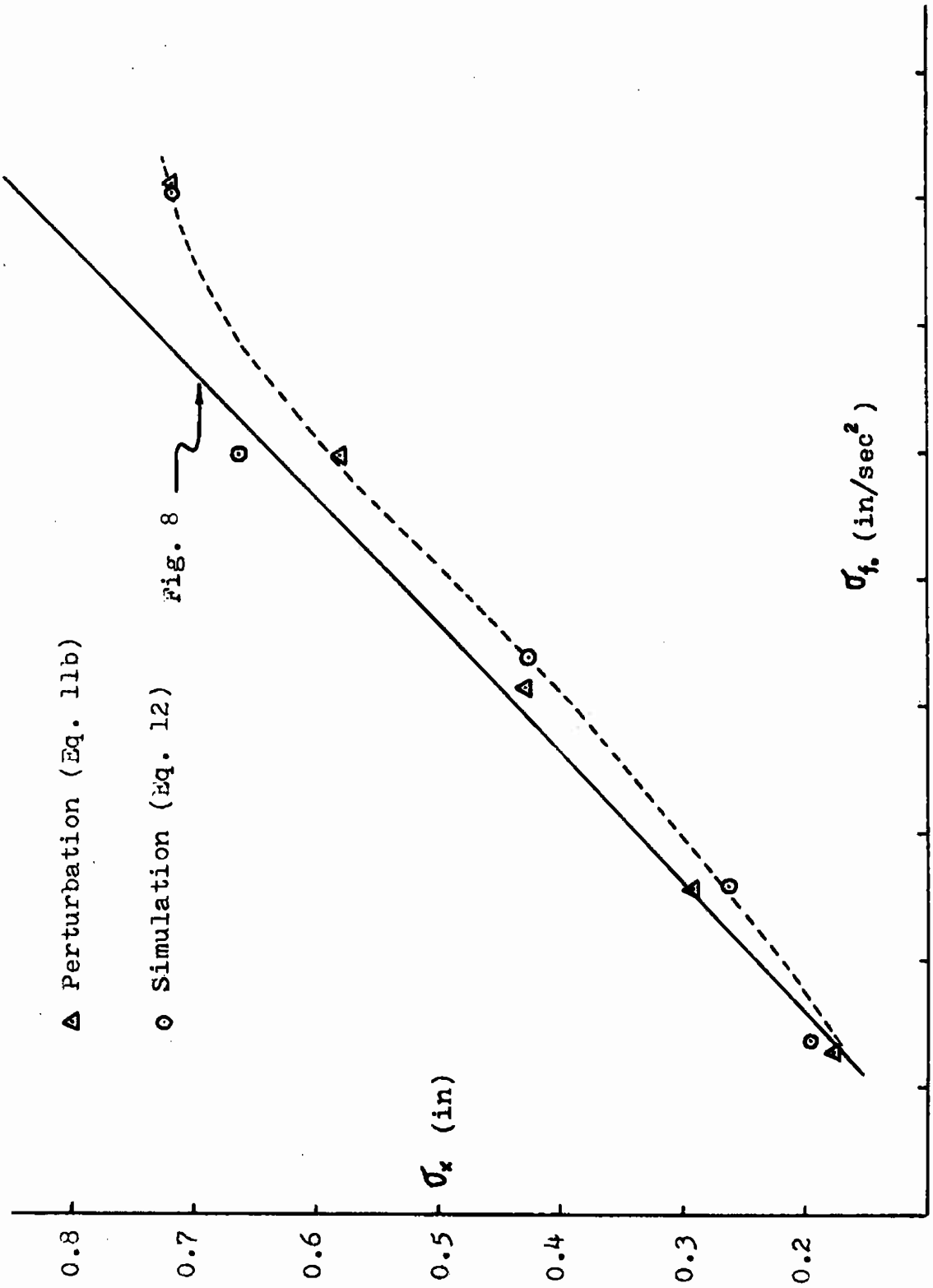

Fig. 12. RMS response of system to excitation with $\zeta = 0.02$ and $u = 0.10$

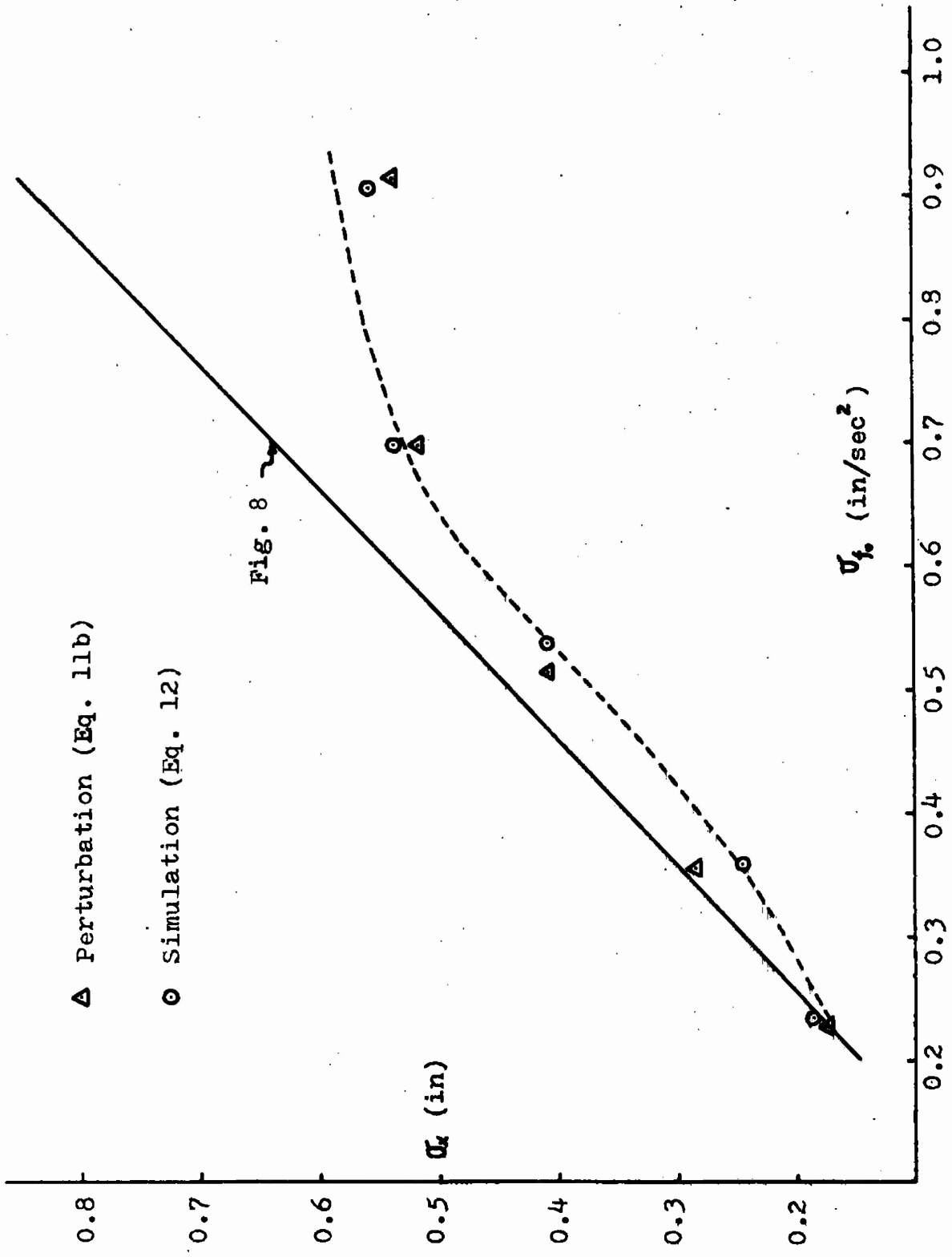

Fig. 13. RMS response of system to excitation with $\zeta = 0.02$ and $u = 0.20$

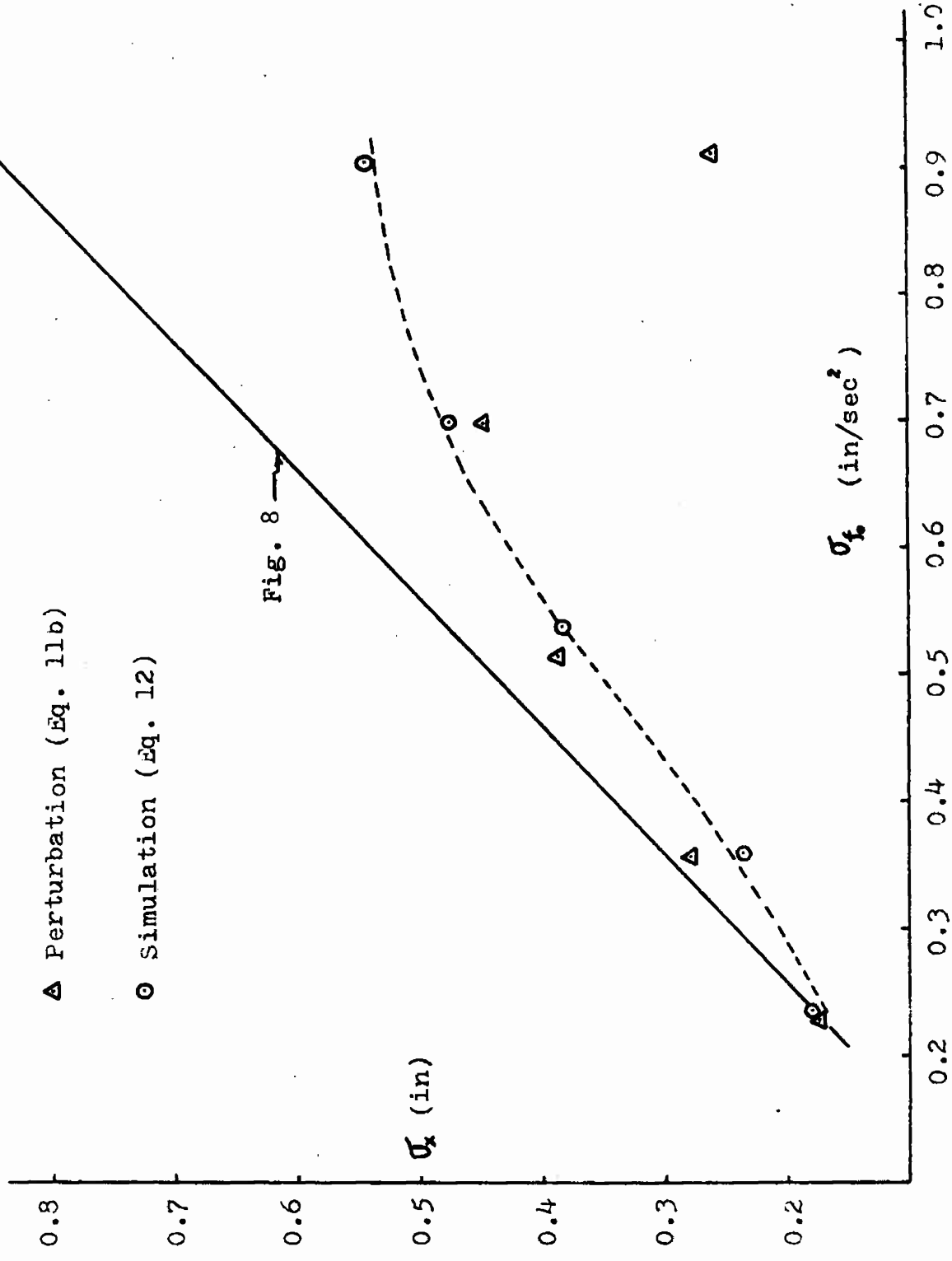

Fig. 14. RMS response of system to excitation with $\zeta = 0.02$ and $u = 0.30$

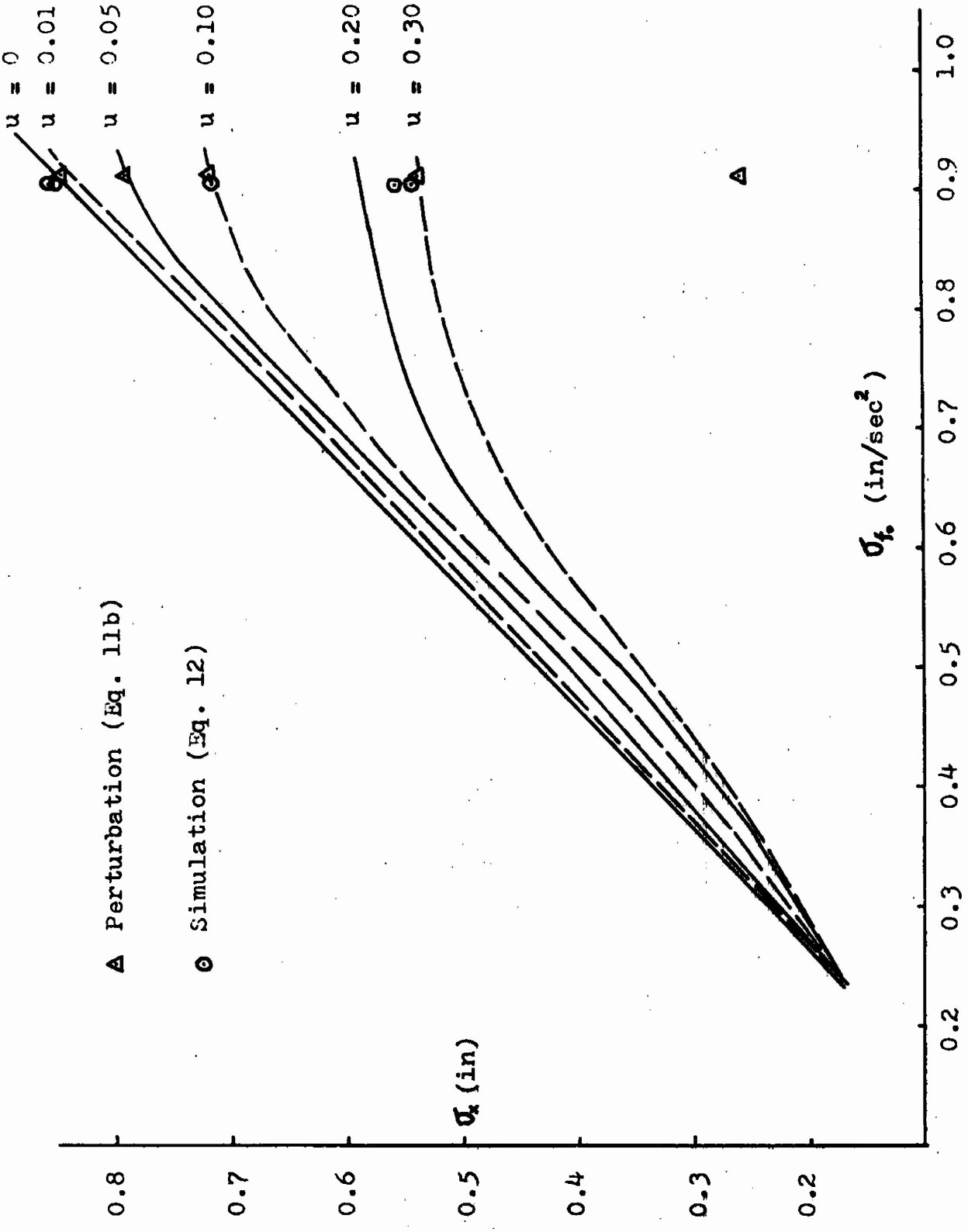

Fig. 15. RMS response of system to excitation with $\zeta = 0.02$

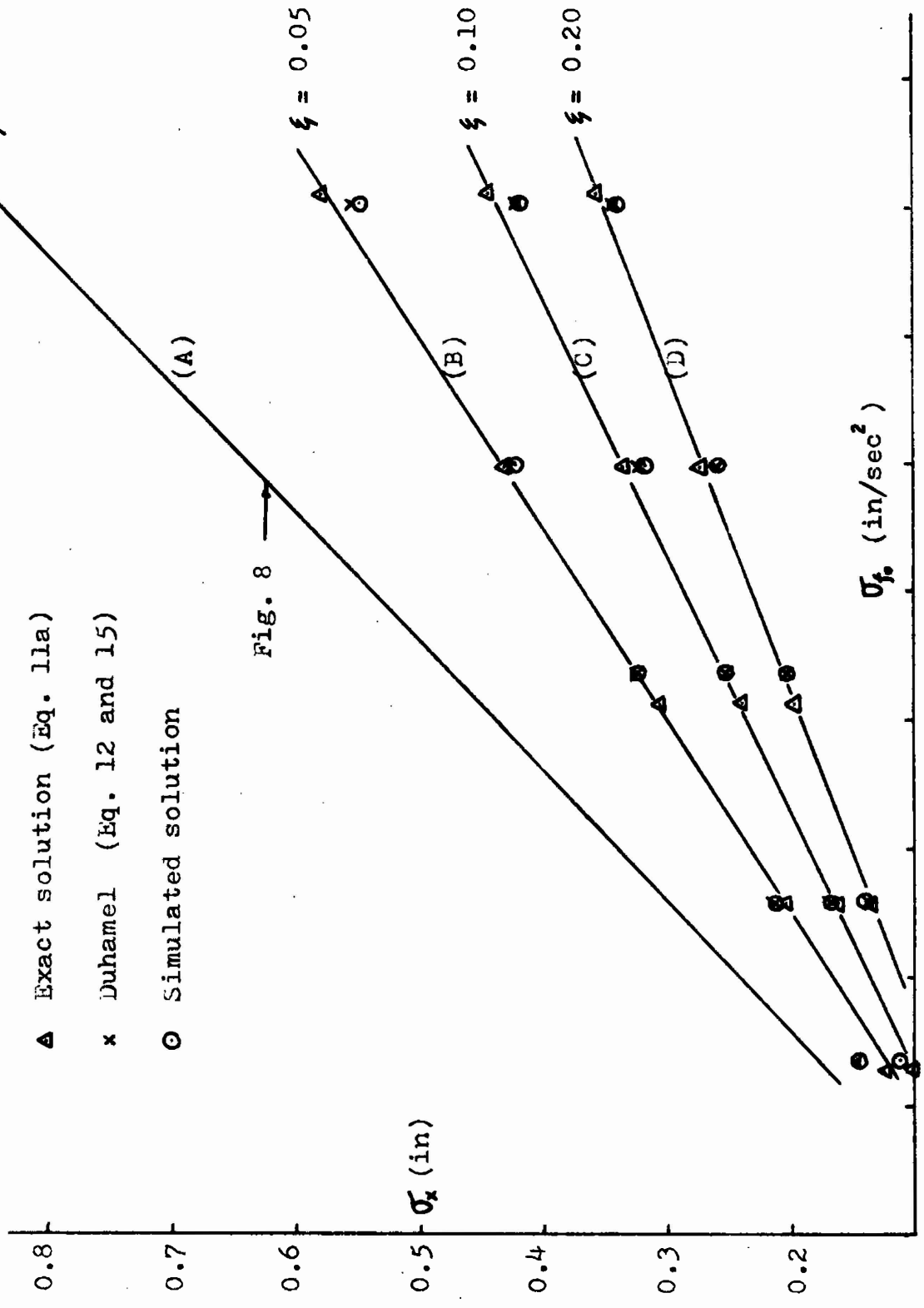

Fig. 16. RMS response of system to excitation with u = 0 (linear system)

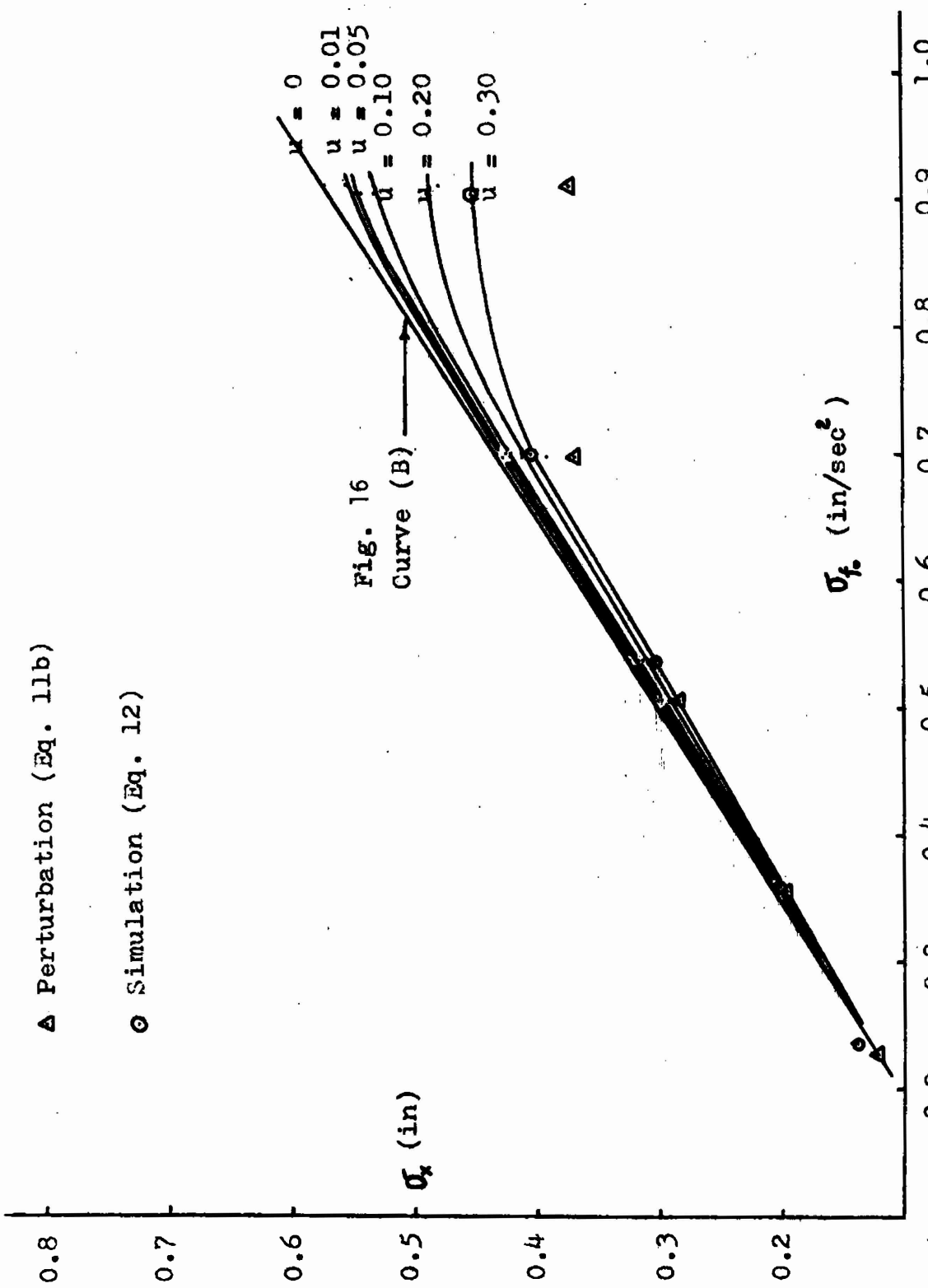

Fig. 17. RMS response of system to excitation with $\zeta = 0.05$

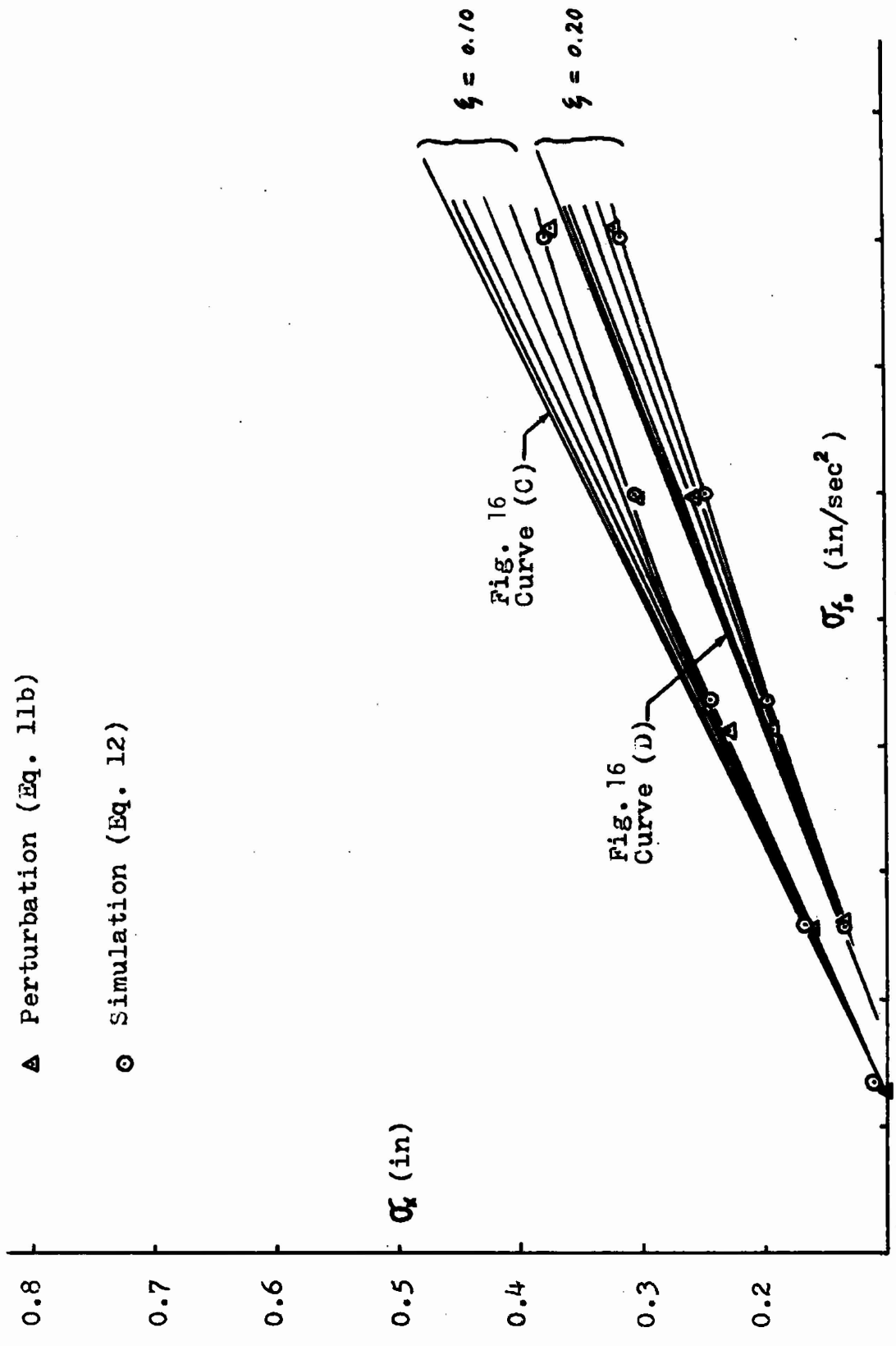

Fig. 18. RMS response of system to excitation with ζ = 0.10 and ζ = 0.20

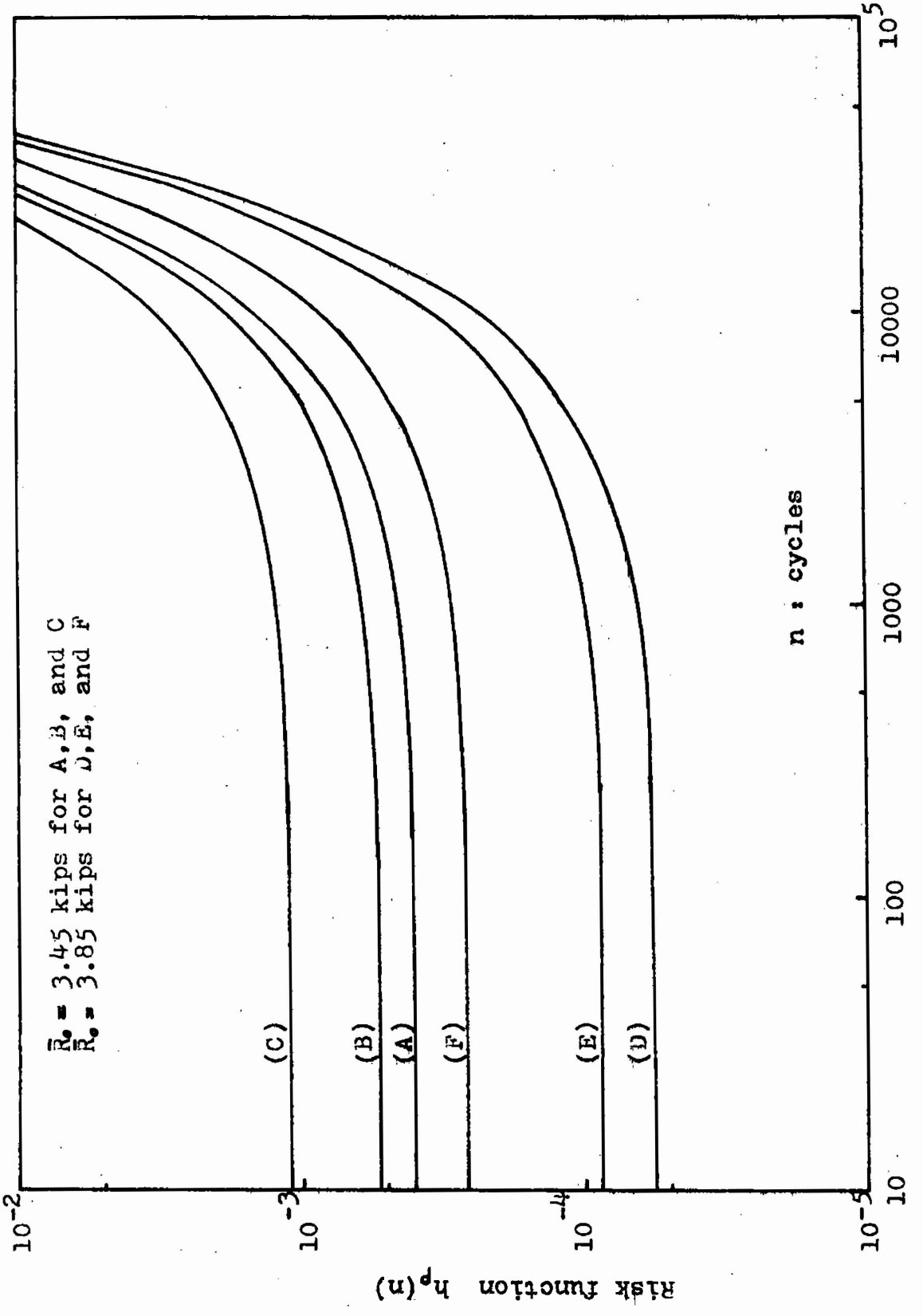

Fig. 19. Risk function as a function of cycles

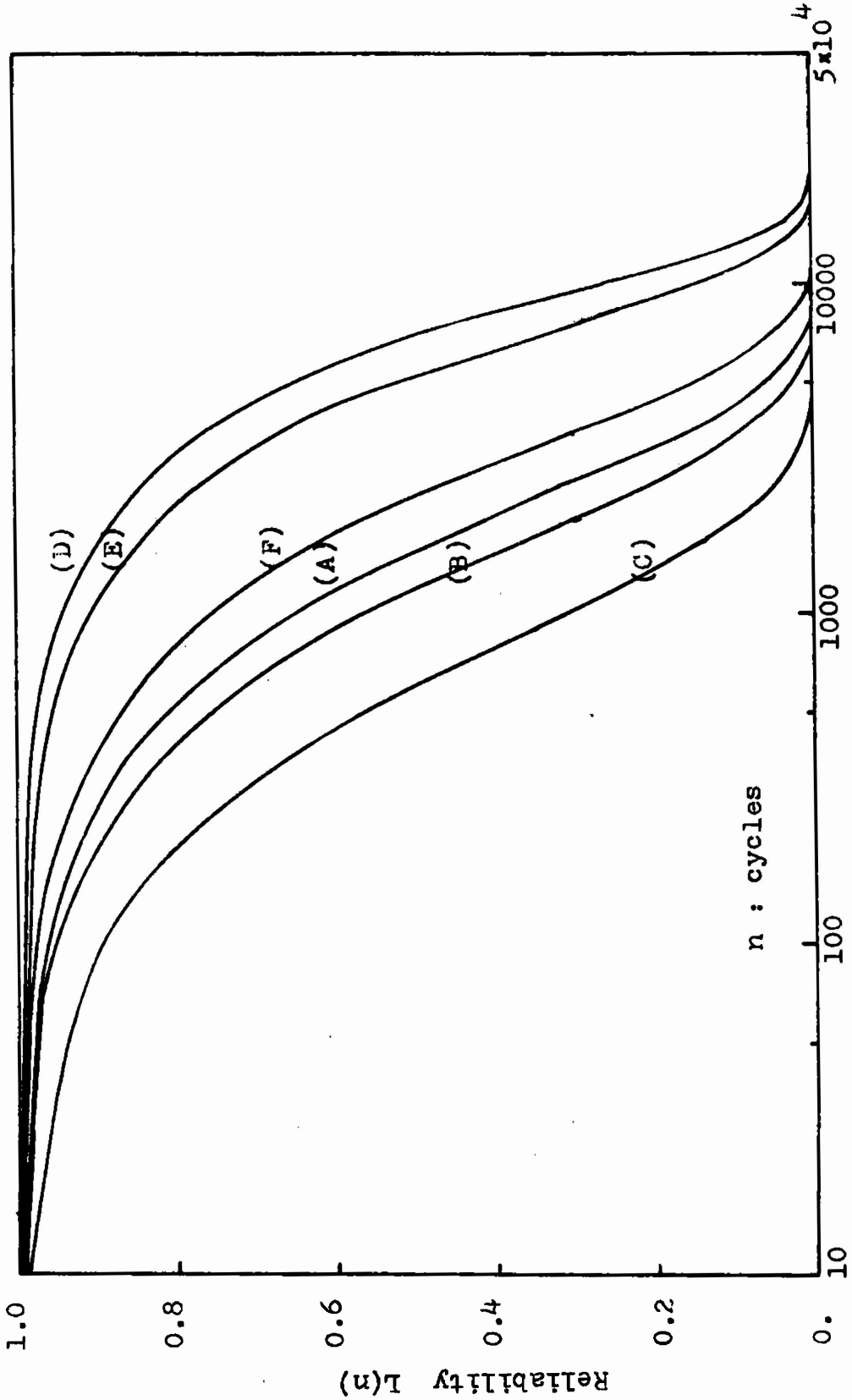

Fig. 20. Reliability of structure as a function of cycles

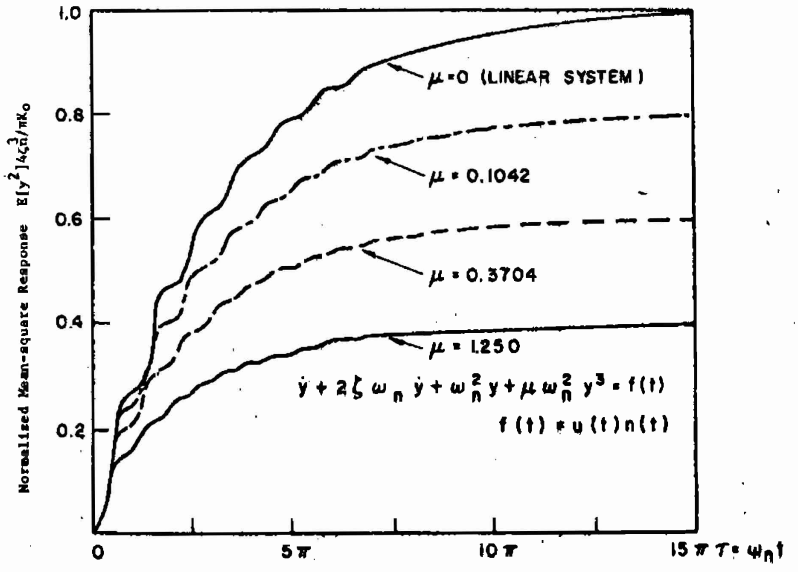

Mean-square Response of the Nonlinear Systems with various Nonlinearities to White Noise Modulated by a Unit Step Function. System Damping $\zeta = 0.05$

Figure 21

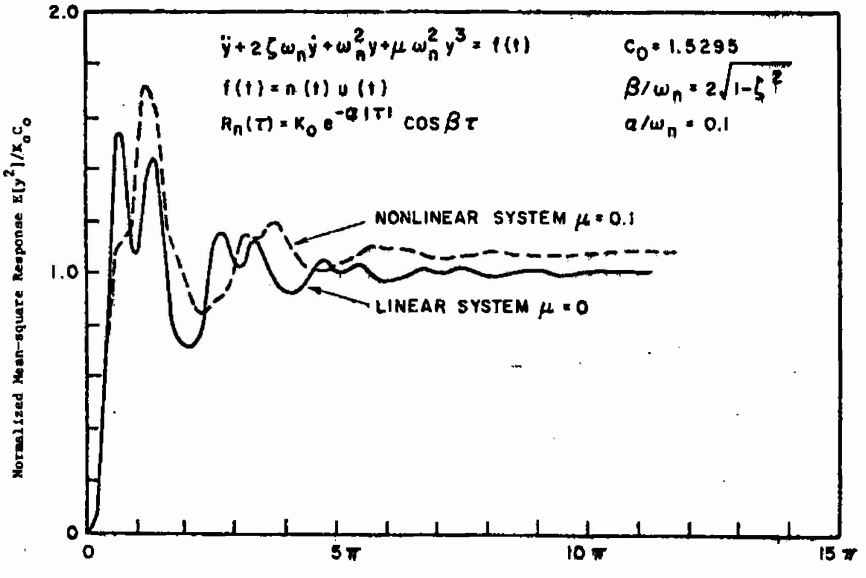

Mean-square Response of the Systems to Correlated Noise modulated by a Unit Step Function. System Damping $\zeta = 0.1$

Figure 22